Megadroughts in the Common Era and the Anthropocene

Benjamin I. Cook[1,2]✉, Jason E. Smerdon[2], Edward R. Cook[3], A. Park Williams[3,4], Kevin J. Anchukaitis[3,5,6], Justin S. Mankin[2,7], Kathryn Allen[8,9,10], Laia Andreu-Hayles[3,11,12], Toby R. Ault[13], Soumaya Belmecheri[6], Sloan Coats[14], Bethany Coulthard[15], Boniface Fosu[16], Pauline Grierson[17], Daniel Griffin[18], Dimitris A. Herrera[19,20], Monica Ionita[21,22], Flavio Lehner[13,23], Caroline Leland[3,24], Kate Marvel[1,25], Mariano S. Morales[26,27], Vimal Mishra[28], Justine Ngoma[29], Hung T. T. Nguyen[3], Alison O'Donnell[17], Jonathan Palmer[10], Mukund P. Rao[3,30,31], Milagros Rodriguez-Caton[31], Richard Seager[2], David W. Stahle[32], Samantha Stevenson[33], Uday K. Thapa[30,33], Arianna M. Varuolo-Clarke[2] and Erika K. Wise[34]

Abstract | Exceptional drought events, known as megadroughts, have occurred on every continent outside Antarctica over the past ~2,000 years, causing major ecological and societal disturbances. In this Review, we discuss shared causes and features of Common Era (Year 1–present) and future megadroughts. Decadal variations in sea surface temperatures are the primary driver of megadroughts, with secondary contributions from radiative forcing and land–atmosphere interactions. Anthropogenic climate change has intensified ongoing megadroughts in southwestern North America and across Chile and Argentina. Future megadroughts will be substantially warmer than past events, with this warming driving projected increases in megadrought risk and severity across many regions, including western North America, Central America, Europe and the Mediterranean, extratropical South America, and Australia. However, several knowledge gaps currently undermine confidence in understanding past and future megadroughts. These gaps include a paucity of high-resolution palaeoclimate information over Africa, tropical South America and other regions; incomplete representations of internal variability and land surface processes in climate models; and the undetermined capacity of water-resource management systems to mitigate megadrought impacts. Addressing these deficiencies will be crucial for increasing confidence in projections of future megadrought risk and for resiliency planning.

The concept of megadroughts came to prominence with research into Common Era (CE; Year 1–present) palaeoclimate droughts over western North America[1–5]. This research documented multi-decadal periods of extreme aridity (or various hydrological deficits[1–5]) before 1600 CE, as well as widespread ecological disturbances[6–8] and societal disruptions[9–12]. Although recurrent and persistent droughts are an intrinsic feature of North American hydroclimate variability, these megadroughts were primarily distinguished by their much greater persistence (for example, multiple decades) than even the most extreme decadal-length instrumental-era droughts during the 1930s and 1950s[13,14].

Since then, extreme droughts across the globe have been increasingly referred to as megadroughts, despite often large differences in their severity, duration, or spatial extent. These include multi-decadal periods of enhanced aridity in Australia[15,16], South America[17], Europe[18], Central Asia[19,20], and Mesoamerica[21]; a multi-season drought in 1540 CE over Europe[22]; spatially extensive multi-year droughts in India[23]; the late Ming Dynasty drought in China[24,25]; and an early twenty-first-century decadal drought in Chile and Argentina[26–28]. As anthropogenic warming is expected to increase drought severity and risk in many regions of the world[29,30], the term has also been increasingly applied to droughts amplified by climate change, both in observations[26,31] and in model projections[32,33].

The use of the megadrought label has therefore been inconsistent, owing partly to an absence of applicable objective criteria that define when a drought becomes a megadrought, or when a period of moisture deficit

✉e-mail: benjamin.i.cook@nasa.gov

https://doi.org/10.1038/s43017-022-00329-1

Key points

- The term 'megadrought' is often used to refer to droughts that exceed the length of most droughts in the instrumental record, the period of climate observations largely serving as the basis for modern water-resource management and infrastructure.
- Although developing a more quantitative megadrought definition is challenging, it is suggested that the term be reserved for "persistent, multi-year drought events that are exceptional in terms of severity, duration, or spatial extent when compared to other regional droughts during the instrumental period or the Common Era".
- Past megadroughts caused major ecological and societal disturbances over the last two millennia and were forced primarily by persistent ocean states, with possible secondary contributions from internal atmospheric variability, volcanic and solar forcing, and land–atmosphere interactions.
- Some of the most active megadrought regions in the past are also areas where anthropogenic climate change is projected to increase future drought risk through declines in precipitation, increases in evaporative demand, and/or changes in plant water use.
- Megadroughts have the potential to substantially strain modern water-management systems, although understanding of the risks of such events, and their ultimate impacts, is still limited by imperfect knowledge of past and future megadrought dynamics.

becomes persistent enough to represent a shift in the mean state (aridification) rather than a discrete transient event (drought). Moreover, although several reviews of megadroughts exist[34–36], these have overwhelmingly focused on North America and predate more recent advances in understanding of natural drought variability and the role of anthropogenic climate change (ACC) in contemporary and future events.

In this Review, we synthesize advances in understanding of megadrought dynamics over the past 2,000 years and into the future from a global perspective, leveraging state-of-the-art palaeoclimate reconstructions, detection and attribution studies, and climate model simulations. We suggest a formal definition for megadroughts, and demonstrate that regions on all continents outside Antarctica have experienced drought intervals in the past that meet the proposed criteria. We summarize evidence that strengthens previous hypotheses that ocean–atmosphere interactions forced many past megadroughts, and discuss how ACC is likely to increase drought risk and severity in many megadrought-prone regions. Finally, we discuss extant uncertainties and knowledge gaps that must be addressed to improve understanding of past megadroughts and increase confidence in projections of future risks and impacts.

Defining megadroughts

Data on droughts over the past 2,000 years are available from proxy-based reconstructions, including lake sediments[37], corals[38], tree rings[39], and multi-proxy efforts[40]. Of particular importance among these datasets are tree ring-derived drought atlases: annually resolved, gridded reconstructions of the summer season Palmer Drought Severity Index (PDSI; a soil moisture index) that cover most of the northern hemisphere[34,41–44], southern South America[45], and eastern Australia and New Zealand[46]. These atlases are valuable tools to understand spatio-temporal drought variability and dynamics during the CE[3,34,42–49].

Author addresses

[1]NASA Goddard Institute for Space Studies, New York, NY, USA.
[2]Division of Ocean & Climate Physics, Lamont-Doherty Earth Observatory, Columbia University, New York, NY, USA.
[3]Tree Ring Laboratory, Biology and Paleo Environment Division, Lamont-Doherty Earth Observatory, Columbia University, New York, NY, USA.
[4]Department of Geography, University of California, Los Angeles, Los Angeles, CA, USA.
[5]School of Geography, Development, and Environment, University of Arizona, Tucson, AZ, USA.
[6]Laboratory of Tree-Ring Research, University of Arizona, Tucson, AZ, USA.
[7]Department of Geography, Dartmouth College, Hanover, NH, USA.
[8]School of Geography, Planning, and Spatial Sciences, University of Tasmania, Hobart, Tasmania, Australia.
[9]School of Ecosystem and Forest Sciences, University of Melbourne, Melbourne, Victoria, Australia.
[10]ARC Centre of Excellence for Australian Biodiversity and Heritage, School of Biological, Earth and Environmental Sciences (BEES), University of New South Wales, Sydney, New South Wales, Australia.
[11]CREAF, Bellaterra, Barcelona, Spain.
[12]ICREA, Barcelona, Spain.
[13]Department of Earth and Atmospheric Sciences, Cornell University, Ithaca, NY, USA.
[14]Department of Earth Sciences, University of Hawaiʻi at Mānoa, Manoa, HI, USA.
[15]Department of Geoscience, University of Nevada, Las Vegas, NV, USA.
[16]Department of Geosciences, Mississippi State University, Starkville, MS, USA.
[17]School of Biological Sciences, The University of Western Australia, Perth, Western Australia, Australia.
[18]Department of Geography, Environment & Society, University of Minnesota, Minneapolis, MN, USA.
[19]Instituto Geográfico Universitario, Universidad Autónoma de Santo Domingo, Santo Domingo, Dominican Republic.
[20] Department of Geography, University of Tennessee, Knoxville, TN, USA.
[21]Paleoclimate Dynamics Group, Alfred Wegener Institute Helmholtz Center for Polar and Marine Research, Bremerhaven, Germany.
[22]Emil Racovita Institute of Speleology, Romanian Academy, Cluj-Napoca, Romania.
[23]Climate and Global Dynamics Laboratory, National Center for Atmospheric Research, Boulder, CO, USA.
[24]Department of Environmental Science, William Paterson University, Wayne, NJ, USA.
[25] Center for Climate Systems Research, Columbia University, New York, NY, USA.
[26] Laboratorio de Dendrocronología e Historia Ambiental, Instituto Argentino de Nivología, Glaciología y Cs. Ambientales, CONICET, Mendoza, Argentina.
[27]Laboratorio de Dendrocronología, Universidad Continental, Huancayo, Peru.
[28]Civil Engineering Department, Indian Institude Technology Gandhinagar, Gandhinagar, Gujarat, India.
[29]Department of Biomaterials Science and Technology, The Copperbelt University, Kitwe, Zambia.
[30]Cooperative Programs for the Advancement of Earth System Science, University Corporation for Atmospheric Research, Boulder, CO, USA.
[31]Department of Plant Science, University of California, Davis, Davis, CA, USA.
[32]Department of Geosciences, University of Arkansas, Fayetteville, AR, USA.
[33]Bren School of Environmental Science and Management, University of California, Santa Barbara, Santa Barbara, CA, USA.
[34]Department of Geography, University of North Carolina at Chapel Hill, Chapel Hill, NC, USA.

Combining updated and existing versions of the drought atlases into a pseudo-global data set enables investigation of the inherent temporal scales of drought variability over the last 600 years (1400–2000 CE) (FIG. 1). Despite differences in regional climate dynamics, summer soil moisture exhibits strong year to year persistence, indicating a tendency for soil moisture anomalies (deficits or surpluses) to carry forward from one year to the next. Positive autocorrelation (unitless) at a 1-year lag is >0.5 for many regions (FIG. 1a), and extends to >0.3 into year 2 in some areas (FIG. 1b), including the North American megadrought regions of the Central Plains, Southwest, and Mexico. One major exception to this global tendency towards strong persistence is the west coast of North America, namely California, where autocorrelation is weak or even negative owing to large inter-annual variability and high-frequency, quasi-cyclic variations in cool-season precipitation[50,51].

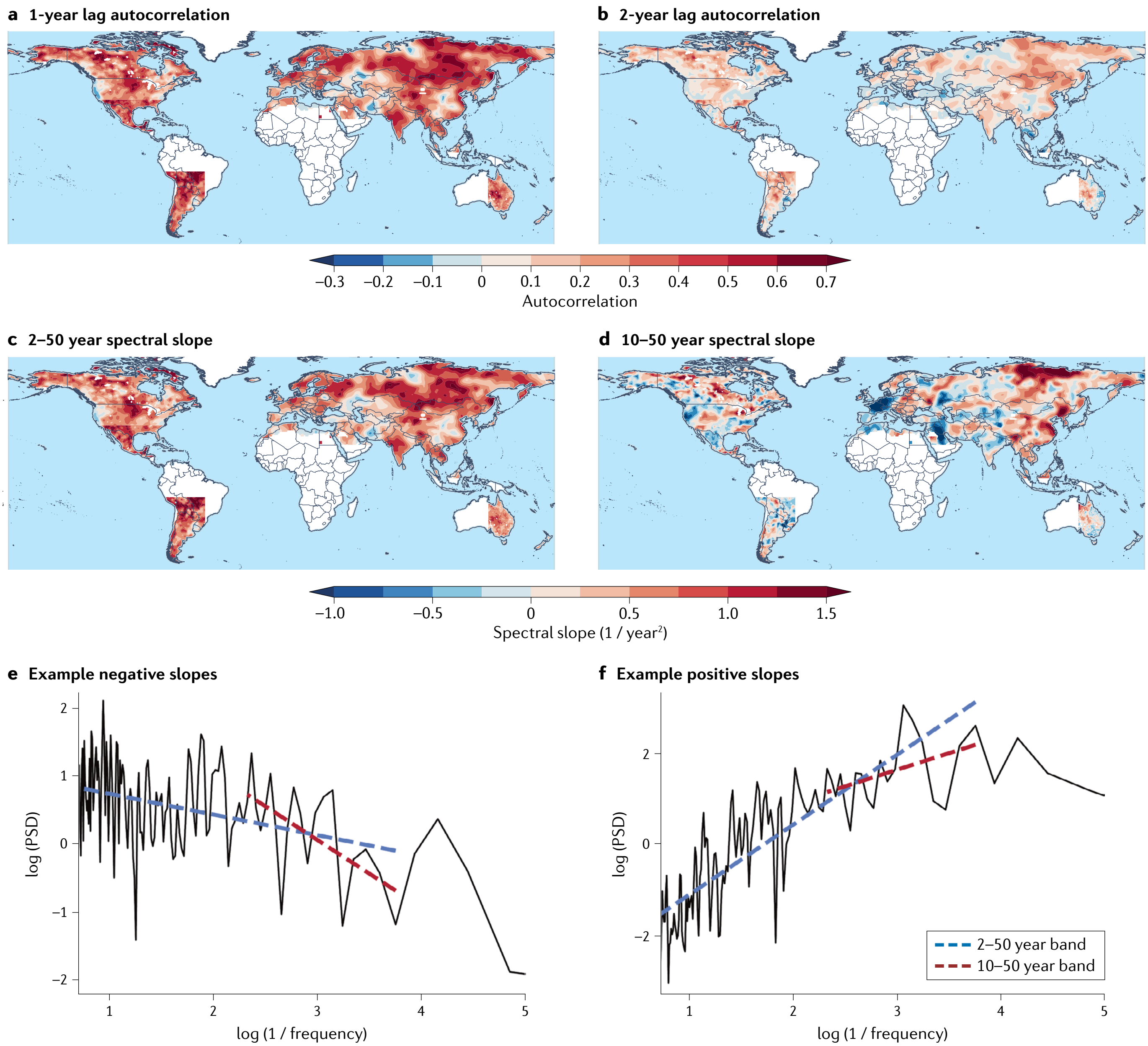

Fig. 1 | **Common Era drought characteristics of soil moisture.** **a**,**b** | Autocorrelation (unitless) of the tree ring-derived drought atlas Palmer Drought Severity Index (PDSI) for 1400–2000 Common Era (CE) at 1 and 2-year lags. **c**,**d** | Slopes (1/year^2) of PDSI power spectral density (PSD), filtered for periodicities of 2–50 years and 10–50 years. Slopes calculated using a least squares regression of the log-transformed power spectral density against the log-transformed periodicity (1/frequency). **e**,**f** | Examples of grid cells with large negative and positive power spectral slopes, with those of the 2–50 year band (blue) and the 10–50 year band (red). Data over North America are from the Living Blended Drought Atlas[34] and the Mexican Drought Atlas[44]. Southern hemisphere reconstructions are from the South American Drought Atlas[45] and the Australia–New Zealand Drought Atlas[46]. Reconstruction over Eurasia is an updated and combined version of the Old World Drought Atlas[42], the European Russia Drought Atlas[41], and the Monsoon Asia Drought Atlas[43]. Analyses of the palaeoclimate record demonstrate that the underlying characteristics of drought variability are highly regional, especially at lower frequencies, highlighting the difficulty of establishing a globally universal definition for megadrought.

The strong persistence of summer soil moisture anomalies and droughts is also evident in power spectra slopes[52–54] (1 / year^2) (FIG. 1c,d). Slopes of the power spectra in the drought atlases filtered for periodicities of 2–50 years are positive across most regions (FIG. 1c), indicating higher proportional variance at lower frequencies and longer timescales. This pattern is consistent with the strongly positive autocorrelation and suggests that extended periods of persistent wetter or drier soil moisture states are common in much of the world. When the power spectra are filtered to remove sub-decadal timescales (focusing on periodicities of 10–50 years), slopes remain positive in some regions, indicating higher power at multi-decadal bands relative to decadal bands (FIG. 1d). These areas include the Central Plains of North America, south-western North America and Central Europe, regions with some of the longest-documented megadroughts in the palaeoclimate record. Consistent with the autocorrelation results, California and the west coast of North America stand out with flat or negative slopes, indicative of variability dominated by higher frequencies.

These regional differences in low-frequency (decadal to multi-decadal) drought variability underscore the difficulty of establishing a universal megadrought definition. For example, although a decade-long drought in California would be highly abnormal given the typical high-frequency (inter-annual) variability in the region, such an event would not stand out as exceptional in Mexico and the south-western USA where decadal variability is larger. Any useful megadrought definition must therefore be contextualized relative to the background drought variability of the region. This cautionary note extends to analyses of megadroughts in climate model simulations, which have the added complication that climate models might have characteristic variability that diverges substantially from the observations.

Defining megadroughts is further complicated by the variety of methods used to determine when an event, whether a drought or megadrought, begins and ends[55,56] (BOX 1). Methods include criteria based on consecutive dry or wet years[57,58]; multi-year to multi-decadal average drought anomalies[32,33,59,60]; methodologies that combine both perspectives[61,62]; or joint criteria that incorporate duration and spatial extent[63]. Thus, analytical choices can strongly affect how megadrought events are defined and discussed, resulting in little consistency across analyses, regions, and time periods.

In recognition of this methodological diversity, and informed by analyses of drought variability, we suggest that megadroughts be defined as persistent, multi-year drought events that are exceptional in terms of severity, duration, or spatial extent when compared with other regional droughts during the instrumental period or the CE. This definition is flexible enough to recognize that different methodologies can be used to define drought or quantify drought characteristics, but also emphasizes that for an event to be considered a megadrought, it must be explicitly compared with other droughts in the available instrumental or palaeoclimate records using the same metrics. Such comparisons are critical for establishing the exceptional nature of a megadrought relative to a long-term baseline and ensuring that the term megadrought refers to the most extreme events, whether they occur in the distant past, the instrumental era, or the future.

Common Era megadroughts

Using our definition, megadroughts can be found on every continent outside Antarctica over the last 2,000 years in the palaeoclimate record (FIG. 2). The evidence for megadrought activity during the CE before the twentieth century is now discussed.

North America. Partly owing to its rich availability of drought-sensitive palaeoclimate archives[2], North America is the most investigated region for megadroughts. Research began in the early twentieth century with the first description of the thirteenth-century megadrought (the 'Great Drought') in the south-western USA[64,65]. Subsequently, multi-centennial periods of low run-off and streamflow in California's Sierra Nevada Mountains were documented from the mid 800s to the mid 1000s, and from the early 1100s to the late 1200s[5]. Palaeo-drought research then advanced rapidly, with evidence of multi-decadal megadroughts across nearly every part of western North America[2,3,34–36] during the entirety of the medieval era and the centuries immediately following[2,34,36] (800–1600 CE). These events include notable megadroughts across the south-western USA during the 1100s and 1200s[36]; in the mid 1100s over the Colorado River Basin[4,66]; and across the south-western USA, Mexico, and Central Plains during the late sixteenth century[8,31,67–69], a drought that includes the driest year (1580 CE) of the last 1,200 years[61].

The effects of these megadroughts are well documented in archaeological, historical, and palaeoecological records. The late 1200s megadrought, for example, likely contributed to the depopulation of the Mesa Verde cliff dwellings in south-western North America (built and occupied by the Ancestral Puebloans for more than 100 years)[64,65,70,71], and possibly the collapse of the Cahokia settlements in the Mississippi River Valley[72]. The late sixteenth-century megadrought, recorded in English and Spanish colonial records[67,73], similarly caused the abandonment of Native American settlements in the south-western USA[74]. More broadly, the megadroughts caused increased wildfire activity[75,76], mass forest mortality events[6–8], and large-scale increases in dune mobilization and dust storm activity[77–80].

Mexico and Central America. In Central America, the most recognized megadrought occurred during the Terminal Classic period, approximately 800–1000 CE. Palaeoclimate records from lakes[37,81–84], speleothems[85], and coastal sediments[86] offer strong evidence for a major extended drought, or multiple drought events, centred over the Yucatán Peninsula and modern-day Guatemala and Belize. Average annual precipitation deficits during the event are estimated to have ranged from 25 to 40%[87] or even from 41 to 54%[88] below average, with peak deficits reaching as high as 52–70%[85,88]. Although debated[89], these hydrological changes are believed to have contributed to the putative 'collapse' of the southern Maya kingdoms.

Box 1 | Defining droughts and megadroughts

Drought and megadrought characteristics are highly sensitive to the calculation of their start and termination dates. This point is demonstrated by applying three different methods of drought-event detection to a single reconstructed soil moisture time series (800–2021 Common Era (CE)) from south-western North America[61]: Williams — defining extended droughts as having at least 10 consecutive years with negative 10-year trailing mean values, trimming the start and end dates to avoid starting or ending the events with consecutive annual (non-smoothed) positive anomalies, and dismissing events shorter than 5 years[61]; Meehl — defining on consecutive, negative 11-year centred mean values[62]; and Coats — beginning droughts with two consecutive negative annual values, continuing the event until two consecutive positive values occur[57].

Focusing on extended (5-year or longer) droughts in the 1,200-year soil moisture reconstruction, the Williams, Meehl and Coats methods identify 30, 41 and 56 events, respectively. Many of the worst megadroughts are detected by all three methods, but often with differences (both minor and major) in their start and end dates. For example, although all three methods find the same start date for the late thirteenth-century megadrought, the event is terminated over a decade earlier for Coats compared with Williams or Meehl (see the figure, panel **a**), and, consequently, the megadrought is much shorter (see the figure, panel **c**) and more moderate (see the figure, panel **d**) when using that methodology. Even larger differences are evident for the late sixteenth-century megadrought (see the figure, panel **b**).

More generally (see the figure, panels **c**,**d**), comparing the different methods reveals that droughts based on the Williams method have longer durations and higher overall severity, those based on the Coats method are shorter because drought termination is easier, and those based on the Meehl method have lower overall severity owing to inclusion of wet years during the beginning or end of the drought. In addition, each of the three methods could lead to varying results depending on the time period used to define baseline conditions when the long-term mean drought anomaly is set to zero. Thus, although there is no clear argument that any of the approaches are superior, a consistent drought definition method is required when comparing drought events, as is an awareness of the underlying assumptions and limitations associated with the chosen methodology. PDSI, Palmer Drought Severity Index.

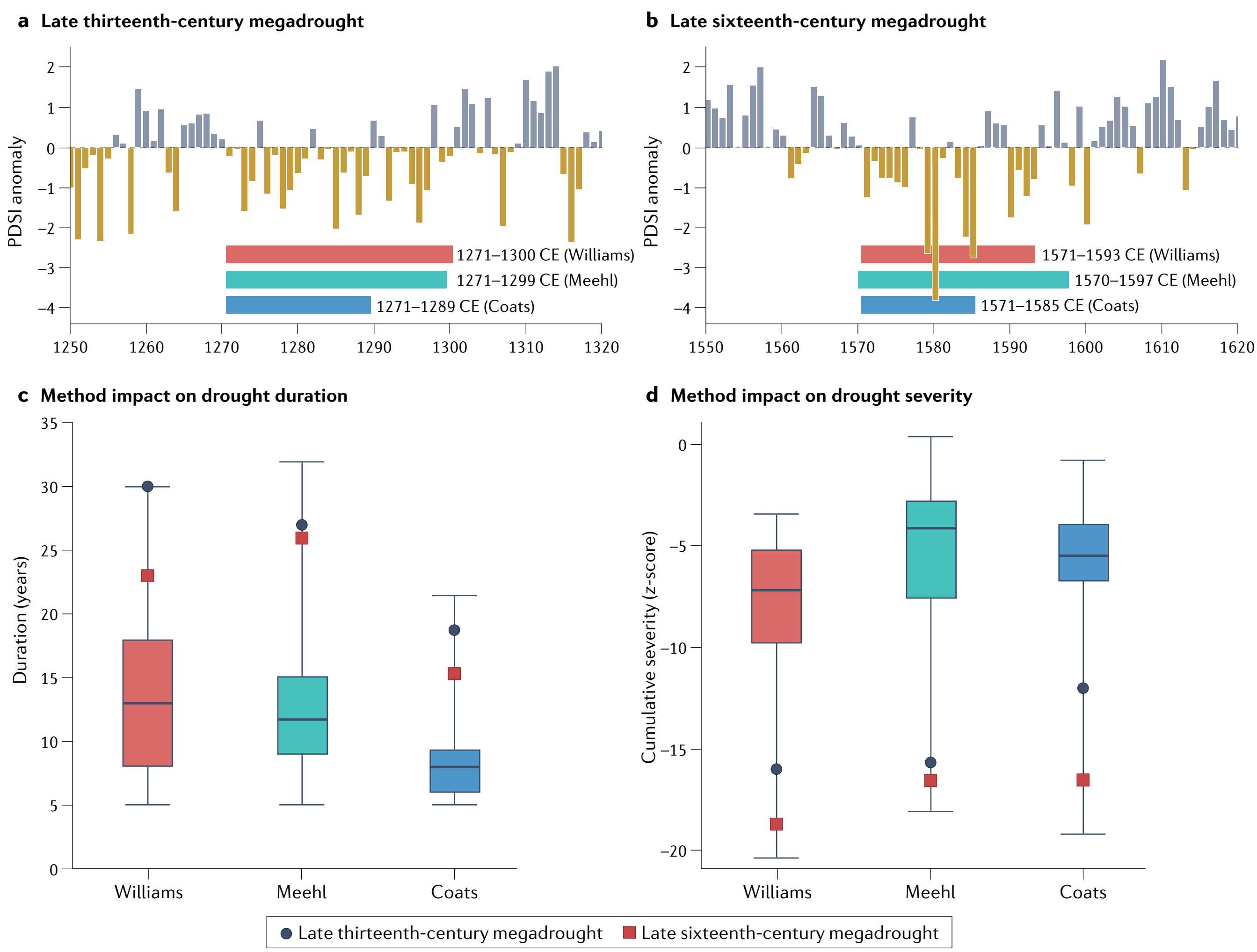

Similarly, there is evidence of megadrought activity in other parts of Mexico, often overlapping with events in the south-western USA and Central America. Major multi-decadal megadroughts affected the Toltec (1149–1167 CE) and Aztec (1378–1404 CE) civilizations[21,44], the former coinciding with the decline of the Toltec capital at Tula. The Terminal Classic megadrought is also believed to have extended into Central Mexico during 897–922 CE. Megadroughts were additionally observed during the Spanish Conquest (1514–1539 CE)[21], followed by a mid 1500s event in central Mexico that predated the late sixteenth-century megadrought in the south-western USA and likely contributed to an outbreak of haemorrhagic fever in 1576 that caused ~2 million deaths[10,67].

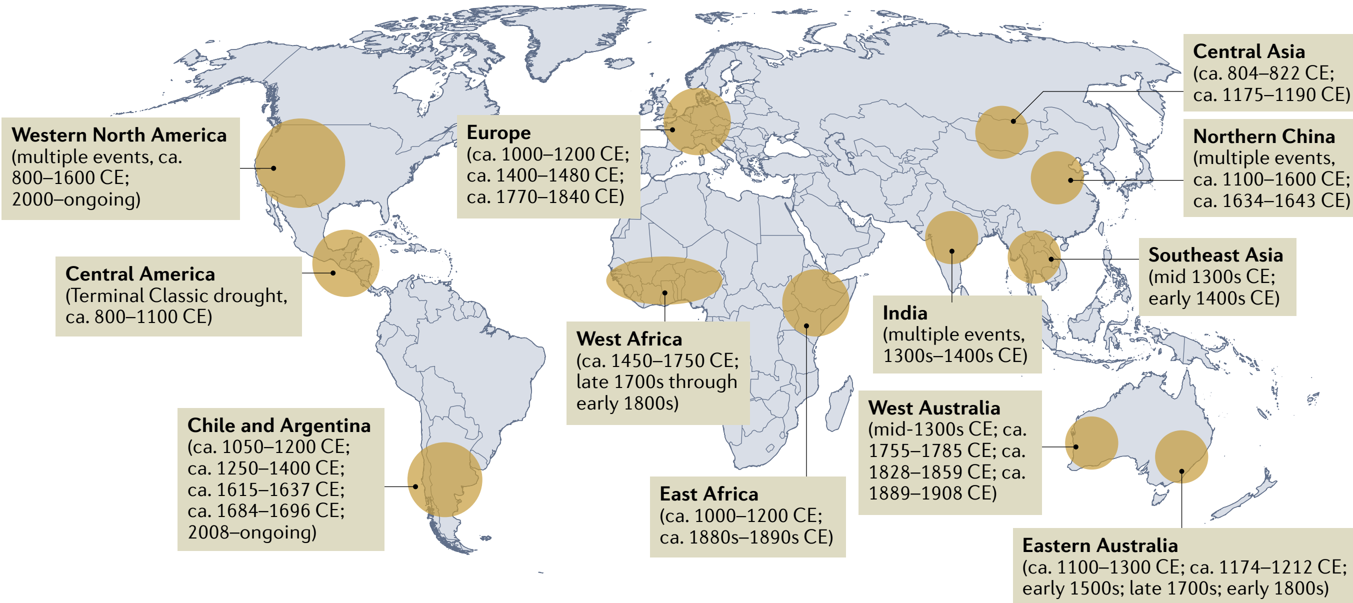

Fig. 2 | **Common Era megadroughts.** Timing of Common Era (Year 1–present) regional megadroughts recorded in observations and the palaeoclimate record. Although there is variability in the timing and recurrence, the palaeoclimate record demonstrates that megadroughts are an intrinsic part of natural hydroclimate variability during the CE, affecting regions on every continent outside Antarctica.

South America. Megadroughts were also commonplace in South America. Patagonia experienced a multi-decadal megadrought at the same time as the first major California megadrought of the CE[5], and seven other distinct medieval era megadroughts in Central Chile were concurrent in time with megadroughts over south-western North America[17]. Subsequent events, however, were not temporally coincident. These include a decadal drought in Patagonia at the end of the fifteenth century[45]; extended periods of enhanced aridity in central Chile and central-western Argentina in the middle of the sixteenth, the eighteenth, and the beginning of the twenty-first centuries[45]; two decadal-scale megadroughts in 1615–1637 CE and 1684–1696 CE; and an extreme 5-year drought in 1800–1804 in the Altiplano region. This latter event is referred to as the 'Silver Mine' drought[90]. Although relatively short in duration, this event was one of the driest and most spatially extensive periods of drought during the ~200-year period of intensive Spanish mining in the region, extending from the Altiplano in Bolivia and into central Argentina[45].

For tropical South America, less detailed information is available on CE hydroclimate. Nevertheless, a 2,300-year lake sediment record from the Central Andes[91] indicates extended periods of reduced South American summer monsoon precipitation during the medieval era and over the last century[91]. Moreover, multi-centennial tree ring-based precipitation reconstructions[92] also highlight prolonged drought periods in the mid nineteenth century and late eighteenth century in the eastern Amazon.

Africa. In Africa, high-resolution CE palaeoclimate records are only sparsely available, challenging efforts to resolve droughts on timescales shorter than several decades or even a century. The exception is in the Mediterranean region of North Africa, where tree rings have been successfully employed to reconstruct frequent and severe multi-decadal droughts during the thirteenth and sixteenth centuries[93]. Outside this area, lake records constitute the primary source for drought reconstructions. However, such records often have limited precision age models and act as low-pass filters on climate signals, making it challenging to identify the timing and severity of major hydroclimate events, particularly before the late eighteenth century. Following this period, information from higher resolution proxies, historical records, and documentary evidence is more widely available.

Despite their issues, lake records highlight several multi-decadal to centennial-scale periods of enhanced aridity over East Africa during 1–1000 CE that could cautiously be interpreted as megadroughts[94–96]. These include persistent periods of low flows into Lake Turkana, and reduced precipitation over the Ethiopian highlands from 200 BCE to 300 CE[97]; reduced rainfall during the first two centuries of the CE at Lake Challa[98]; and several multi-decadal droughts at Lake Edward between 400 and 890 CE[99]. East Africa was especially dry during the medieval era, with substantial megadroughts recorded in declining lake levels between 1000 and 1250 CE[98,100,101].

From the late eighteenth century through to the first half of the nineteenth century[102,103], nearly the entire continent transitioned into a major episode of aridity. These decades were some of the most arid in East Africa of the last 1,000 years, with exceptional declines recorded at multiple lakes[98,102,104,105]. Another major drought followed in the 1880s and 1890s over Ethopia[102,106,107], causing severe famine from 1888 to 1892 (REF. [108]).

In other parts of Africa, an approximately 300-year megadrought is evident in West Africa from 1450 to 1750 CE, likely the driest in the region during the late Holocene[109–113]. Megadroughts also affected the Sahel and Guinea Coast in 1765–1780 CE and 1789–1798 CE[114].

Europe and Asia. Europe experienced several multi-century megadroughts over the past 2,000 years. These include an event in Central Europe from the mid 400s to 600 CE[115,116] and another in Germany and Fennoscandia from 1000 to 1200 CE[42]. The duration and magnitude of the latter event were similar to the California megadroughts that occurred from the early 800s to the late 1000s[5,34]. Two further centennial-scale events occurred in Central Europe during the Spörer (1400–1480 CE) and Dalton (1770–1840 CE) solar minima[18]. Within these periods, particularly intense multi-decadal droughts[42] were recorded over north-central Europe during 1437–1473 CE and 1779–1827 CE, with 1798–1808 CE being especially dry over England and Wales. In addition, the western Mediterranean experienced several decades of severe drought in the mid 1600s, as recorded in tree-ring reconstructions[117] (1620–1640 CE) and documentary proxies from Catalonia[118] (1626–1650 CE). Over the Iberian Peninsula, extended drought also occurred from 1680 to 1700 CE, the coldest interval of the Little Ice Age during the Maunder Minimum, and from 1760 to 1800 CE[119].

A series of multi-decadal megadroughts are evident in India during the fourteenth and fifteenth centuries, associated with 20–30% declines in monsoon rainfall, including at least one event that was 30 years long[120,121]. Megadroughts occurred in Southeast Asia around the same time, most notably two multi-decadal events in the mid 1300s and early 1400s that might have contributed to the collapse of the Angkor civilization in modern-day Cambodia[122] (BOX 2). Decadal-scale megadroughts occurred regularly in northern China[123], including during 1146–1155 CE, 1240–1249 CE, 1483–1492 CE, 1578–1587 CE, and 1634–1643 CE. The seventeenth-century drought contributed to widespread famine that led to the deaths of 20 million people and is widely believed to have helped motivate the peasant uprising that ended the Ming Dynasty[124]. In arid

Box 2 | **The Angkor drought**

Within tree-ring based regional average soil moisture reconstructions[43], the Angkor drought stands out as an especially severe, persistent and spatially extensive event in Southeast Asia (see the figure, panels **a**,**b**). Using a simple drought definition requiring at least 5 consecutive dry years, 21 total extended drought periods are identified — of which the Angkor drought is the longest, spanning 24 years from approximately 1344 to 1367 Common Era (CE). Moreover, the event was the third most spatially extensive extended drought, with negative 24-year mean soil moisture anomalies affecting 89% of the regional land area. The single most severe soil moisture deficit of any extended drought also occurred during the Angkor drought in 1363 CE, although the time-average soil moisture anomaly ranks as the fourth driest overall (see the figure, panel **c**). Thus, based on these analyses and megadrought-defining characteristics, this event qualifies as a megadrought, exhibiting exceptional severity, duration, and spatial extent compared with other droughts in the region over the last ~800 years.

The Angkor megadrought triggered a series of events that contributed to the demise of the Angkor civilization[122]. During this megadrought, streamflow in the Mekong was approximately two or three standard deviations below normal[258], causing Angkor's rulers to seal off reservoirs to minimize water losses. The modified infrastructure had much less hydraulic capacity and was subsequently heavily damaged by a severe flood in 1375 CE[122,258]. With this loss of water storage capacity, Angkor could not sustain itself during the next major drought (approximately 1399–1404 CE) and flood sequence. Consequently, much of the Greater Angkor region was eventually abandoned. PDSI, Palmer Drought Severity Index.

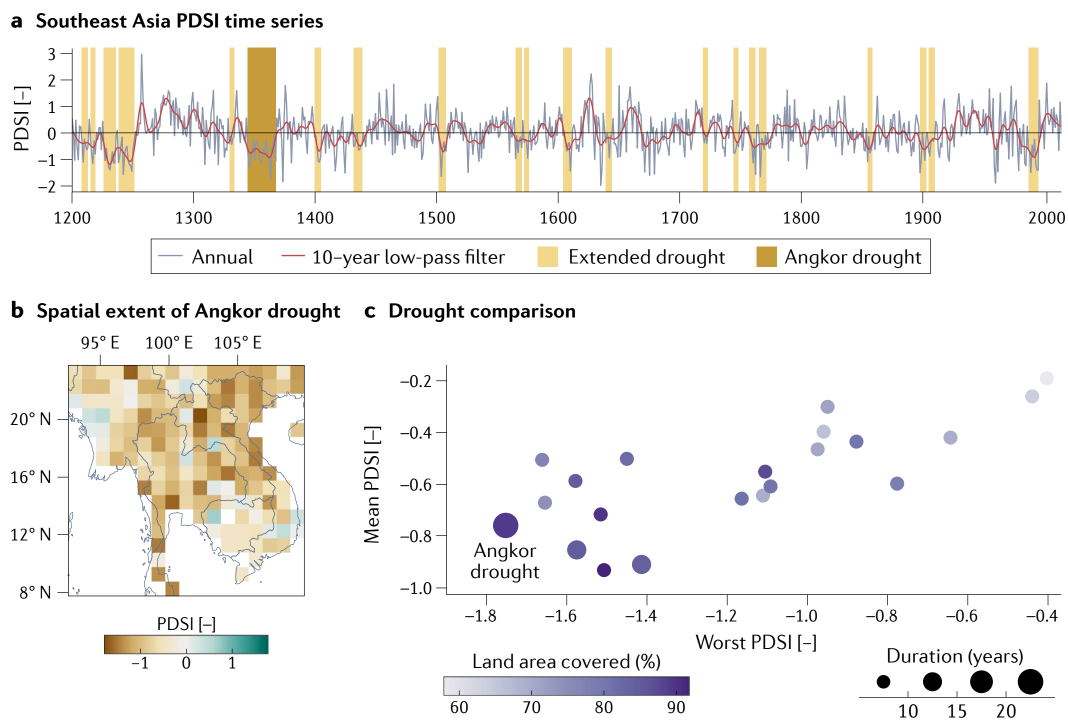

Central Asia, tree-ring chronologies provide evidence for a severe 16-year megadrought from 1175 to 1190 CE, a turbulent period characterized by warfare on the Mongolian steppe, as well as a longer and more intense 19-year megadrought starting in 804 (REFS.[19,20]).

Although most of the extreme megadroughts in Asia have been regionally focused, extreme multiregion events also occurred. These include the 'Strange Parallels' drought from 1756–1768 CE that affected peninsular India, Southeast Asia, and central Russia[43] and the Great Victorian drought from 1876–1878 CE that affected India, Southeast Asia, and China[43,125,126]. The latter event, occurring during the height of British global colonialism, contributed to widespread famine, 12.2–29.3 million deaths in India and 19.5–30 million deaths in China[127].

Australia. Much like Africa, mainland Australia has very few local palaeoclimate proxies with sufficient temporal resolution to develop detailed estimates of CE drought variability. Consequently, most hydroclimate reconstructions use non-local proxies, assuming some degree of stationarity in climate teleconnections and covariability across regions. Examples include tree rings from Tasmania and New Zealand[46], ice cores from Antarctica[128], and corals along the east coast of Australia[38]. More recently, however, advances have been made to develop local proxy records, including new tree-ring reconstructions in Western Australia that extend back over 600 years[15].

Ice core records suggest that south-western Australia was especially drought-prone in the mid 1300s[128] and during the eighteenth and nineteenth centuries. Tree-ring records corroborate some of these events, indicating major multi-decadal megadroughts in 1755–1785 CE, 1828–1859 CE, and 1889–1908 CE[15]. The coincidence of the tree ring-derived 1828–1859 CE megadrought in western Australia with coral-derived evidence of low streamflow in Queensland (the lowest in the region since the 1600s[38]) suggests this event might have been especially widespread[15].

In south-east Australia there is further evidence of multiple extended periods of drought, including multi-centennial periods of aridity during the twelfth and thirteenth centuries[129,130] and major decadal-scale megadroughts in the early 1500s, late 1700s and 1820s–1840s[46,131–134]. The region also experienced moderately dry summer conditions from 1550 to 1600 CE, and a more severe but shorter dry period from 1670 to 1704 CE[135]. The central coast in eastern Australia (South East Queensland) also experienced eight major megadroughts over the last millennium[16,136], including a 39-year event from 1174 to 1212 CE[16].

CE palaeoclimate research has produced an ever-expanding body of literature documenting megadroughts on every continent outside Antarctica. It is, therefore, clear that megadroughts are not a phenomenon unique to the regional climate dynamics of western North America but are, instead, an intrinsic part of CE climate variability. Consequently, their global ubiquity strongly suggests that megadroughts are connected to fundamental, and globally important, climate system processes.

Drivers of Common Era megadroughts

Although instrumental and palaeoclimate records are useful for documenting global megadrought activity, deriving information on the driving processes from these data is more difficult. When analysed in conjunction with drought reconstructions, however, climate models can provide complementary insights into the three key hypotheses regarding megadrought causes: external forcing, ocean–atmosphere dynamics, and land–atmosphere interactions. Each of these aspects is now discussed.

External forcing. Many CE megadroughts occurred during periods of anomalous solar and volcanic forcing, motivating hypotheses that external forcing changes are a key driver of global megadrought activity[17,24,82,104,137]. For example, megadroughts in western North America are temporally clustered during the medieval era[2,3], a period of enhanced solar output and reduced volcanic activity[138]. Solar and volcanic forcing are proposed to affect megadrought occurrence through several mechanisms, including increased local temperature responses that enhance evaporative demand[40]; reduced land–sea temperature gradients that weaken monsoons[123,139]; and forced sea surface temperature (SST) changes in regions with teleconnections that cause regional drought[18,48,60,140,141].

However, evidence for the impact of these forcings on megadroughts is mixed. For example, whereas the temporal clustering of North American megadroughts is higher than predicted from random noise alone, the evidence that this clustering was specifically caused by external forcing is much weaker[142,143]. Moreover, hydroclimate responses to forcings vary spatially, as demonstrated by volcanic eruptions being linked to drought in some regions[144] (tropical Africa) and pluvial periods in others[145–147] (Mediterranean, Southeast Asia). Finally, although some climate models can generate megadroughts in response to external forcing[17,24,40,60], they can also generate megadroughts analogous to those in the palaeoclimate record through internal variability alone[57,58,148–150].

Atmosphere–ocean dynamics. Regional hydroclimate variability often results from complex interactions between the ocean and atmosphere. Persistent SSTs, arising from both large thermal inertia and slowly varying ocean circulations, create diabatic heating anomalies in the atmosphere which, in turn, generate atmospheric wave trains, shift storm tracks and modify mean circulation features. These changes subsequently cause droughts, pluvials, or floods in distant regions[151] which, owing to the persistence and slow evolution of SST anomalies, can also be long-lived.

The tropical Pacific and Atlantic are especially important given their strong inter-annual to multi-decadal SST variability and ability to drive teleconnections that influence climate worldwide[151]. Indeed, the influence of the tropical ocean can cause persistent hydroclimate states that would be unlikely to be sustained by atmospheric dynamics alone[17,40,152,153]. The temporal concurrence of spatially separate hydroclimatic events — a pattern also unlikely to occur only through stochastic atmospheric variability — further implicates SSTs as a common driver of CE megadroughts. For instance, Pacific SST variability is linked to the co-occurrence of the late sixteenth-century megadrought in south-western North America and a major pluvial in eastern Australia[68], as well as concurrent megadroughts in North and South America throughout the palaeo-record[5,17,154]. Climate models can also generate megadroughts in response to low-frequency variations in Pacific and Atlantic SSTs that have similar characteristics to events in the palaeoclimate record[17,40], even if the timing is inconsistent with observations[57,154].

In the Pacific, decadal-scale cold SST anomalies in the eastern tropical Pacific have been identified as the primary cause of many medieval era megadroughts in North America[40,153] and South America[17]. Cold tropical Pacific SSTs cool the tropical atmosphere and displace the jet streams and storm tracks in each hemisphere poleward[155]. Additionally, Rossby wave teleconnections create anomalous high pressure in the extratropical Pacific, west of North and South America[154]. This pattern resembles the atmospheric response to inter-annually varying La Niña conditions, diverting precipitation-bearing storms poleward of the drought regions[154]. Conversely, warm central Pacific SSTs, often related to positive phases of the Interdecadal Pacific Oscillation, have been strongly linked to megadroughts in eastern Australia[16,46,130] and Asia[43] as the locus of convection in the Indo-Pacific sector shifts east. Megadroughts in eastern China have also been linked to western Pacific SST variability driving a weakening of the East Asia summer monsoon[156].

SST variability outside the Pacific has also been linked to megadrought occurrence. Warm SSTs across the Atlantic sector likely contributed to megadroughts in North America[40], in West Africa in approximately 1000–1200 CE and 1500–1700 CE[112], and in Central America during the Terminal Classic period[157]. Cold SSTs in the North Atlantic, by contrast, are related to megadroughts in Central Europe[18]. The Indian Ocean can also contribute to multi-decadal drought, especially when acting synergistically with west Pacific SSTs[93,158].

There are uncertainties regarding the extent to which these megadrought-related SST and corresponding large-scale circulation states were externally forced[17,18,40,48] or are a consequence of exceptional periods of internal climate variability[57,149]. For example, the dynamical thermostat mechanism has been invoked to explain how enhanced radiative forcing (increased solar output and weak volcanism) during the medieval era could have shifted the eastern tropical Pacific into a persistent cold state[140,141], increasing megadrought risk in western North America. This mechanism, induced by increased radiative forcing from rising anthropogenic greenhouse gas concentrations, might be responsible for the observed shift in tropical Pacific SST gradients since the mid twentieth century that have contributed to the ongoing megadrought in south-western North America[61,159,160]. Notably, this trend is counter to the weakened SST gradient projected by most global climate models[159], and it is uncertain what proportion of these SST trends is forced or a consequence of internal ocean–atmospheric variability[57,149,160].

Land–atmosphere interactions. Land–atmosphere interactions can also substantially affect drought severity and persistence. Declining soil moisture during drought conditions increases sensible heat fluxes and decreases latent heating and evapotranspiration[161]. Warmer temperatures and reduced atmospheric moisture from these changes at the land surface can then amplify surface drying by increasing atmospheric aridity and evapotranspiration[162] or suppressing precipitation[161], although not in all cases[163]. Additional feedbacks occur through declines in vegetation health and coverage and increases in wind erosion or dust aerosols[164], which also reduce energy availability and evapotranspiration through similar mechanisms. Land–atmosphere interactions are strong in many megadrought-prone regions[162,165], and such processes likely contributed to many historical droughts, including the Dust Bowl of the 1930s[166] and the multi-decadal Sahel drought from the 1970s to the early 1990s[167].

There are at least two megadroughts in which land–atmosphere interactions are thought to have had a role. During the medieval era megadroughts over the Central Plains of North America, geomorphological evidence indicates that declines in vegetation coverage caused high levels of wind erosion and dust storm activity[80]. Climate simulations suggest these changes would have significantly increased summer temperatures and suppressed early summer precipitation[168], enhancing the severity and persistence of the simulated megadroughts compared with simulations using SST forcing alone[168]. In the case of the Terminal Classic megadrought in Central America from 800 to 1000 CE, widespread deforestation (forest conversion to cropland) might account for a substantial fraction of the total precipitation deficit[87]. Using an empirically constrained estimate of Pre-Columbian land use[169], models suggest that deforestation could have caused a 10–20% reduction in late summer precipitation, contributing to an overall 5–15% decline in annual precipitation across southern Mexico and the Yucatán[169]. Other, more idealized experiments simulated a 15–30% reduction in July precipitation with complete deforestation of Mesoamerica[170].

Although some uncertainties remain, the strongest available evidence strongly implicates tropical SSTs as the primary natural driver of CE megadrought activity in many regions, with possible secondary contributions from external climate forcings and land–atmosphere interactions. Given the robustness of these natural processes.

Climate change and megadroughts

Anthropogenic climate change affects drought risk and severity through forced changes in precipitation[171–173], snow[174,175], and evaporative demand and evapotranspiration[176,177]. Increases in evaporative demand are predominantly caused by warmer temperatures and decreases in relative humidity[31,61,178,179], with these effects at least partially counteracted by reductions in near-surface wind speeds[180]. Plants also respond to changes in climate and atmospheric carbon dioxide concentrations in ways that could either diminish[181] or increase[182,183] evapotranspiration and drought impacts, although the net effect of these competing mechanisms is uncertain.

Through these processes, ACC has intensified soil moisture droughts in California[184,185] and south-western North America[31]; snow and streamflow droughts across the western United States[186–192]; and precipitation droughts in the Mediterranean[193–195], Central America[196], the Caribbean[197], Chile[26], southern Africa[198,199], and south-western Australia[193,200]. Included among these are ongoing events that can be considered megadroughts in south-western North America[61] and central Chile and central-western Argentina[26]. These two events are now discussed, along with consideration of how megadrought risk might change in the future.

The south-western North America megadrought. Beginning in 2000 CE[61,178] and extending at least through the summer of 2022 (the time of this writing), south-western North America has experienced drought conditions that are unprecedented back to 800 CE[31,61]. A regional soil moisture reconstruction ranks 2000–2021 CE as the driest 22-year soil moisture anomaly (-0.87σ) of the last 1,200 years[61]. This event is only comparable with the multi-decadal megadroughts that afflicted the region before 1600 CE, slightly edging out the second driest 22-year soil moisture anomaly (-0.83σ) from 1571 to 1592 CE during the late sixteenth-century megadrought. This extended drought has caused severe declines in water resources[61,201,202], major economic and agricultural losses[203], and widespread wildfire activity[204,205].

Precipitation deficits during this event are strongly influenced by natural variability[160,206] and there is no obvious evidence of a downward trend in precipitation in the region over the last century. One important driver of the precipitation reductions contributing to the twenty-first-century megadrought is a change towards the cool (or negative) phase of Pacific decadal variability at the turn of the century and its persistence thereafter[160,206,207]. This shift is analogous to prior decadal changes in tropical Pacific SSTs that caused large-scale precipitation deficits and drought over the south-west, such as occurred during the 1950s and past megadrought periods.

However, although the natural precipitation deficits alone would have established twenty-first-century drought conditions in the south-west, the region has also experienced significant increases in vapour pressure deficit owing to warmer temperatures and increasing vapour pressure deficits[208–210]. The warming is largely attributable to anthropogenic forcing[179,209], resulting in increased surface water losses that have amplified soil moisture deficits during this drought. Indeed, ACC is believed to account for nearly half (~42%) of the soil moisture deficit during 2000–2021 CE[61].

The large contribution of ACC is also evident in the spatio-temporal evolution of the observed megadrought (FIG. 3a,b). In the absence of anthropogenic forcing, 2000–2021 would have likely been composed of two distinct droughts with more moderate cumulative soil moisture deficits up through 2021 (REF.[61]). Moreover, with anthropogenic effects removed, the most extreme soil moisture deficits would have been localized in southern California and Arizona, consistent with the drought pattern expected of predominantly cool-phase conditions in the tropical Pacific, rather than the more spatially extensive observed drying. Anthropogenic climate change therefore likely turned what would have been a serious, but spatially and temporally constrained, drought with characteristics typical of historical variability in the region into the most severe and widespread megadrought of the last 1,200 years[61].

The Chile–Argentina megadrought. Since 2008, Chile and Argentina have experienced extreme decadal-scale drought conditions. In this region, such persistent droughts are rare, motivating its labelling as a megadrought[26,27,211]. Indeed, the megadrought stands out as exceptional in both the historical record and palaeoclimate reconstructions of the last millennium (FIG. 3c,d). It is the longest consecutive run of drier than normal years during the twentieth century[26], and also the driest, or near driest, decadal-scale drought over the past 1,000 years[26,27,211,212]. Precipitation deficits during the megadrought reached 20–40%[26,27,213] below normal in some locations and years, causing 7–25% reductions in lake areal extent[214], up to 90% declines in streamflow[27,215], and major impacts on snow and glaciers in high alpine areas[27,216]. As a result, the megadrought has severely affected water resources[27,215,217], wildfire[218], and vegetation health[27] across the region.

As with south-western North America, decadal variations in tropical Pacific SSTs are an important natural driver of the current megadrought. However, there is some evidence that ACC is intensifying the precipitation deficits[193,219]. For instance, anthropogenic greenhouse gas emissions and stratospheric ozone depletion have contributed to positive trends in the Southern Annular Mode and poleward expansions in the southern hemisphere Hadley Cell, shifting storm tracks and the jet stream and reducing precipitation over extratropical South America. Anthropogenic warming has also contributed to warmer ocean temperatures in the subtropical south-west Pacific Ocean, which might have amplified ridging and drying over the region[28], further reducing regional precipitation. Collectively, these anthropogenically modified processes are estimated to explain 20–50% of the total precipitation reductions during the Chile–Argentina megadrought[26,27,213,220].

The future of megadrought risk. Many of the most megadrought-prone regions during the CE are locations expected to experience increased drought severity and risk with at least ‘medium confidence’[221]. These include western North America, Central America, the Caribbean Islands, Europe and the Mediterranean, Chile, and southern Australia. Such changes are expected to occur in response to season-specific precipitation declines[222,223], decreases in snowpack storage[174,192,224,225], and increases in evaporative demand[226] and plant water use[182,183]. In part because of relatively uncertain

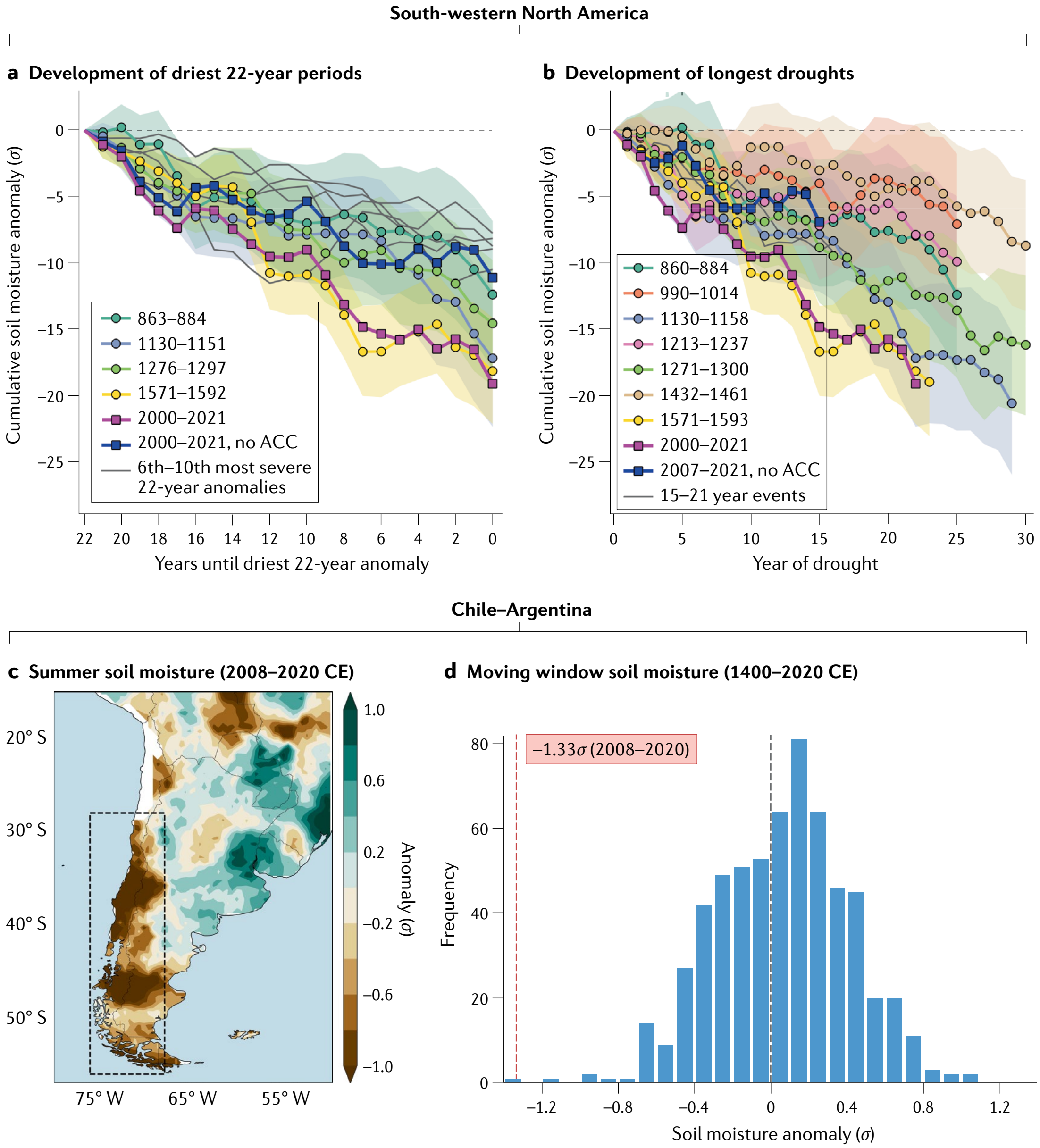

Fig. 3 | **Anthropogenic contributions to twenty-first-century megadroughts. a** | Cumulative summer season soil moisture anomalies over south-western North America associated with the driest 22-year mean anomalies in the soil moisture reconstruction[61] (800–2021 Common Era (CE)). Shading represents the 95% confidence bounds in reconstructed values. In the blue line, the effects of anthropogenic climate change (ACC) on the 2000–2021 soil moisture anomalies have been removed. **b** | As in part **a**, but cumulative soil moisture anomalies associated with the development of all droughts at least 15 years in length. The magnitude of the observed 2000–2021 CE drought is 66% higher and the onset date 7 years earlier compared with the version where ACC effects are removed, highlighting the strong contribution of climate change to this event. **c** | Observed summer (December–February) soil moisture anomalies[257] for southern South America for 2008–2020 CE. **d** | Reconstructed and observed 13-year moving window soil moisture anomalies for 1400–present CE[45]. Dashed red line indicates soil moisture anomalies for the 2008–2020 period. In central/southern Chile and Argentina, the 2008–2020 CE regional average soil moisture for 2008–2020 CE ranks as the single driest 13-year period during the last 600 years. Panels **a** and **b** adapted, with permission, from REF.[61], Springer Nature Limited.

regional precipitation responses in climate models, in most regions increased drought risk occurs as a direct response to warming-induced declines in snow and increases in evapotranspiration[29,222]. A notable exception is in the Mediterranean-climate regions of South America, the Mediterranean Sea, southern Africa, and south-western Australia, where increased drought risk is caused by robust reductions in cool-season precipitation related to anomalous high pressure occurring within an adjustment of planetary-scale stationary waves[193,227].

In line with increases in overall drought risk, CMIP6 simulations forced with a moderate warming scenario (SSP2–4.5) indicate that many of the CE megadrought regions will experience substantial increases in multi-decadal megadrought risk in the latter half of the twenty-first century (FIG. 4). This finding is supported

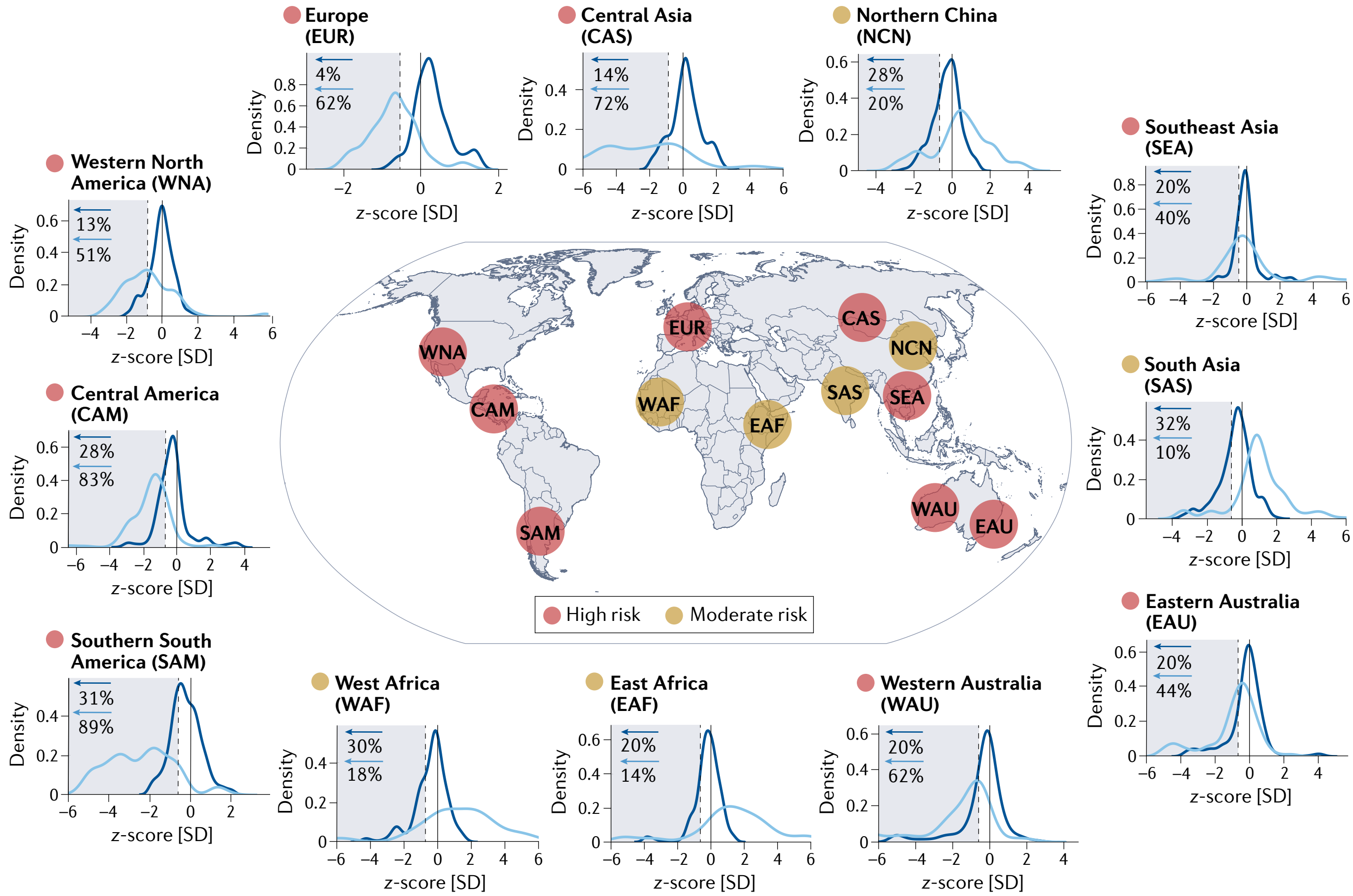

Fig. 4 | **Projected megadrought risk.** Regional density distributions of multi-model ensemble 21-year mean standardized total column soil moisture for the late twentieth (1951–2000 Common Era (CE); dark blue) and late twenty-first (2051–2100 CE; light blue) centuries. The multi-model ensemble is produced from 22 models (Supplementary Table 1) under a moderate warming (SSP2–4.5) scenario, with soil moisture standardized to a baseline period of 1851–1950 CE. 'Megadrought risk' (percentages) represents the fraction of 21-year mean soil moisture anomalies in the pooled ensembles that are drier than the fifth percentile (vertical grey dashed line) estimated during the 1851–1950 CE baseline. On the map, regions of 'high risk' in the late twenty-first century (red circles) experience mean shifts in the multi-model ensemble towards drier conditions (for example, western North America, Europe, Central America), whereas those with 'moderate risk' (orange circles) typically experience small increases in megadrought risk associated with subsets of models rather than any coherent ensemble-mean shift (for example, West Africa, northern China). SD, standard deviation.

by several climate model ensembles which, under a high-emissions scenario (RCP 8.5), suggest that soil moisture mean states in many regions (including western North America, western Europe, southern Africa, and Australia) would meet or exceed megadrought definitions for the entirety of the twenty-first century[228]. Western North America is one of the most vulnerable regions: analyses using the previous generation of climate models (CMIP5) document a 60–80% likelihood of decadal (11-year) and multi-decadal (35-year) megadroughts occurring over the south-west and Central Plains of the USA by the end of the twenty-first century under both moderate and high warming scenarios[33]. Similarly, CMIP6 simulations suggest an ~50% increase in the likelihood of events analogous to the 2000–2020 CE south-western North America megadrought occurring by the end of the twenty-first century across low, medium, and high warming scenarios[59].

If realized, these changes would likely mean an unprecedented level of megadrought activity compared with even the most arid centuries of the Common Era. However, there is evidence that lower forcing scenarios would partially mitigate increases in megadrought risk and severity[32,59], as increases in risk are attributable to background trends and shifts in the mean state which scale strongly with the magnitude of forcing, rather than changes in decadal or multi-decadal hydroclimate variability[228]. Moreover, projected megadrought risks for regions such as the south-western USA remain sensitive to internal climate variability, even under high forcing. Large initial condition ensembles of climate simulations are therefore necessary to better constrain uncertainties in future regional megadrought risk estimates[229,230]. Climate mitigation is thus likely to offer critical benefits for moderating megadrought severity and risk, even if future increases cannot be entirely avoided.

Summary and future perspectives

Megadroughts are distinguished by their exceptional nature compared with more typical droughts in the instrumental or palaeoclimate records. By this definition, megadroughts have occurred on every continent outside Antarctica during the CE, and have been most strongly linked to SST variability, especially in the tropical Pacific and Atlantic basins. Anthropogenic climate change has already amplified the severity of contemporary megadroughts in south-western North America, and in central Chile and central-western Argentina; it is projected to further increase future megadrought risk to largely unprecedented levels by the end of the twenty-first century. Such events would probably present substantial challenges to water resources[201] and ecosystem resilience[231]. Even so, climate mitigation is likely to reduce event risk and severity compared with the most extreme warming scenarios[32].

Despite progress in understanding natural and anthropogenic megadrought drivers, confidence in projections of megadrought risk is partially undermined by uncertainties in estimates of natural drought variability. This uncertainty is especially true for regions where hydroclimate proxy coverage during the CE is sparse (for example, the Amazon), where there is heavy reliance on remote proxies (for example, mainland Australia), or where most information comes from archives (for example, lake records) with low resolution and substantial time uncertainties (for example, sub-Saharan Africa before the late 1700s). These limitations make it difficult to fully constrain natural drought variability, the past occurrence of megadroughts, and the characteristics of these events. Addressing these limitations will require prioritizing new efforts to collect and develop seasonally and annually resolved proxies in historically poorly sampled regions, and then synthesizing these new records into spatially resolved reconstructions. Climate models introduce additional uncertainties. Climate models generally underestimate natural hydroclimate variability, and might therefore underestimate future megadrought risk[52,53,232], and often disagree on projected changes in atmospheric circulation and precipitation[233]. Although it is difficult to know what changes are needed to improve these models, more comprehensive evaluations against the much longer palaeoclimatic record would probably offer insights into where and why the models are failing.

With temperature having an increasingly important role in modern and future droughts[18,234–240], past megadroughts are likely to be imperfect analogues of future events. Whereas historical megadroughts were caused by precipitation deficits, higher temperatures are an increasingly important contributor to soil moisture, streamflow, and snow drought risk and severity. For example, anthropogenic warming allowed the megadrought at the turn of the twenty-first century to emerge across a broad swath of south-western North America, even though drought-promoting circulation anomalies were likely more severe and persistent during the megadroughts that occurred before 1600 CE, when anthropogenic forcing of the global climate was minimal [61]. These warmer temperatures are likely to amplify drought impacts on ecosystems[6,241], although by how much is unclear owing to the complex and uncertain responses of vegetation to climate and atmospheric carbon dioxide concentrations[181–183]. Much of this uncertainty is centred on the representation of land surface and vegetation processes within climate models, which are often highly parameterized and simplified. Moving forward, it will be critical to understand and improve how these process representations affect model sensitivities, mean states, fluxes, and the underlying manifestation of drought events[242].

Water management further complicates the picture of how future droughts and megadroughts are likely to affect human water resources, demand, and consumption. Activities such as surface reservoir storage and management, irrigation, and sustainable groundwater management are all invaluable interventions that can increase drought resilience[202,243–246]. However, it is unclear whether current implementations of these policies will be sufficient to adapt to a warmer and drier future, especially because adaptive capacities have generally not been tested in the context of megadroughts. In the case of the ongoing megadrought in south-western North America, unsustainable groundwater withdrawals[202,247] and record-breaking lows in reservoir storage at Lake Powell and Lake Mead[61] suggest that current policies are inadequate[248,249]. In some cases, management activities could even be maladaptive or have unintended consequences. For example, increases in irrigation efficiency can reduce streamflow and groundwater recharge because run-off is reduced as water is increasingly allocated to evapotranspiration, often eliminating expected increases in total water availability[250]. Similarly, reliance on reservoir storage can create situations of higher demand and over-reliance, increasing vulnerability to droughts[251].

To address these future challenges, more explicitly considering megadroughts in drought planning exercises will be required. Many water-resource management plans centre on what is often termed the 'drought of record', usually the single worst drought event in the historical record designed to represent a potential worst-case scenario for drought resiliency planning. Texas, for example, uses the 1950s drought as their drought of record[252,253], an event that led to the creation of the Texas Water Development Board and new reservoir construction across the state[252,254]. Given the much more persistent and severe megadroughts in the palaeoclimate record and model projections, however, a more informed approach would be to use palaeoclimatic records to define new droughts of record[39,130] or, at least, develop model exercises to assess how current plans would fare under the much more extreme conditions associated with the megadroughts[255,256]. These approaches are already being considered or applied to water-resource management in California, the Colorado River Basin, and the Missouri River Basin. Such exercises should also consider that a megadrought-prone future could mean shorter or less frequent wet intervals that can limit recovery between droughts, especially for groundwater and larger reservoirs. These issues are already beginning to manifest in the western USA, where persistent and frequent drought periods have impeded groundwater and reservoir recovery during the short intervening wet intervals[61,202,247].

Megadroughts are already stressing adaptive capacities in south-western North America and Chile–Argentina, and it is plausible or even likely that other regions will experience a major megadrought in the coming decades, with similar impacts on water resources. One challenging aspect of these future events will be that much of the increased megadrought risk will occur because of a shift in regional climates to more arid mean states[228] characterized by higher temperatures and, in some cases, reduced precipitation. In some of these regions, megadrought might effectively become the new climate normal, a permanent shift towards drier conditions[201,228] that requires rethinking how droughts are defined given that they are, by definition, temporary events. Regardless, the palaeoclimate record and model projections can be used to better constrain and contextualize these future changes in hydroclimate, droughts, and megadroughts, informing adaptation and allowing for more proactive development of resiliency plans to reduce the impact of these events.

Data availability

North America, Mexico, South America and Australia–New Zealand drought atlas reconstructions are available from http://drought.memphis.edu/. Updated version of the Eurasian drought atlases is available from https://www.dropbox.com/s/vl9jfm7ls0szbin/GEDA_rec.nc. Data for the south-western North America megadrought analyses (BOX 1) can be found at https://www.ncei.noaa.gov/access/metadata/landing-page/bin/iso?id=gov.noaa.nodc:0241207. Data for the Angkor megadrought analysis (BOX 2) can be found at https://www.dropbox.com/s/n2lo99h9qn17prg/madaV2.nc. All CMIP6 data are available from the Earth System Grid (https://esgf-node.llnl.gov/search/cmip6/).

1. Stockton, C. W. & Jacoby, G. C. *Long-term Surface-water Supply and Streamflow Trends in the Upper Colorado River Basin: Based on Tree-ring Analyses* (Institute of Geophysics and Planetary Physics, Univ. of California, 1976).
2. Woodhouse, C. A. & Overpeck, J. T. 2000 years of drought variability in the central United States. *Bull. Am. Meteorol. Soc.* **79**, 2693–2714 (1998).
3. Cook, E. R., A, W. C., Mark, E. C., M, M. D. & W, S. D. Long-term aridity changes in the western United States. *Science* **306**, 1015–1018 (2004).
4. Meko, D. M. et al. Medieval drought in the Upper Colorado River Basin. *Geophys. Res. Lett.* https://doi.org/10.1029/2007GL029988 (2007).
5. Stine, S. Extreme and persistent drought in California and Patagonia during mediaeval time. *Nature* **369**, 546–549 (1994).
6. Williams, A. P. et al. Temperature as a potent driver of regional forest drought stress and tree mortality. *Nat. Clim. Change* **3**, 292–297 (2013).
7. Brown, P. M. & Wu, R. Climate and disturbance forcing of episodic tree recruitment in a southwestern ponderosa pine landscape. *Ecology* **86**, 3030–3038 (2005).
8. Swetnam, T. W. & Betancourt, J. L. Mesoscale disturbance and ecological response to decadal climatic variability in the American Southwest. *J. Clim.* **11**, 3128–3147 (1998).
9. Benson, L. V. & Berry, M. S. Climate change and cultural response in the prehistoric American Southwest. *KIVA* **75**, 87–117 (2009).
10. Acuna-Soto, R., Stahle, D. W., Cleaveland, M. K. & Therrell, M. D. Megadrought and megadeath in 16th century Mexico. *Emerg. Infect. Dis.* **8**, 360–362 (2002).
11. Douglass, A. E. Dating Pueblo Bonito and other ruins of the Southwest. *Natl Geogr. Soc. Contrib. Tech. Papers Pueblo Bonito Ser.* **1**, 1–74 (1935).
12. Stahle, D. W. & Dean, J. S. in *Dendroclimatology: Progress and Prospects* (eds Hughes, M. K., Swetnam, T. W. & Diaz, H. F.) 297–327 (Springer Netherlands, 2011).
13. Schubert, S. D., Suarez, M. J., Pegion, P. J., Koster, R. D. & Bacmeister, J. T. On the cause of the 1930s dust bowl. *Science* **303**, 1855–1859 (2004).
14. Heim, R. R. A comparison of the early twenty-first century drought in the United States to the 1930s and 1950s drought episodes. *Bull. Am. Meteorol. Soc.* **98**, 2579–2592 (2017).
15. O'Donnell, A. J., McCaw, W. L., Cook, E. R. & Grierson, P. F. Megadroughts and pluvials in southwest Australia: 1350–2017 CE. *Clim. Dyn.* **57**, 1817–1831 (2021).
16. Vance, T. R., Roberts, J. L., Plummer, C. T., Kiem, A. S. & van Ommen, T. D. Interdecadal Pacific variability and eastern Australian megadroughts over the last millennium. *Geophys. Res. Lett.* **42**, 129–137 (2015).
17. Steiger, N. J., Smerdon, J. E., Seager, R., Williams, A. P. & Varuolo-Clarke, A. M. ENSO-driven coupled megadroughts in North and South America over the last millennium. *Nat. Geosci.* **14**, 739–744 (2021).
18. Ionita, M., Dima, M., Nagavciuc, V., Scholz, P. & Lohmann, G. Past megadroughts in Central Europe were longer, more severe and less warm than modern droughts. *Commun. Earth Environ.* **2**, 61 (2021).
19. Pederson, N., Hessl, A. E., Baatarbileg, N., Anchukaitis, K. J. & di Cosmo, N. Pluvials, droughts, the Mongol Empire, and modern Mongolia. *Proc. Natl Acad. Sci.* **111**, 4375–4379 (2014).
20. Hessl, A. E. et al. Past and future drought in Mongolia. *Sci. Adv.* **4**, e1701832 (2018).
21. Stahle, D. W. et al. Major Mesoamerican droughts of the past millennium. *Geophys. Res. Lett.* **38**, e2010GL046472 (2011).
22. Pfister, C. in *Historical Disaster Experiences: Towards a Comparative and Transcultural History of Disasters Across Asia and Europe* (ed. Schenk, G. J.) 155–185 (Springer International, 2017).
23. Mishra, V. & Aadhar, S. Famines and likelihood of consecutive megadroughts in India. *npj Clim. Atmos. Sci.* **4**, 59 (2021).
24. Chen, K. et al. One drought and one volcanic eruption influenced the history of China: the Late Ming Dynasty mega-drought. *Geophys. Res. Lett.* **47**, e2020GL088124 (2020).
25. Gao, L. et al. The unusual recent streamflow declines in the Bailong River, north-central China, from a multi-century perspective. *Quat. Sci. Rev.* **260**, 106927 (2021).
26. Garreaud, R. D. et al. The Central Chile mega drought (2010–2018): a climate dynamics perspective. *Int. J. Climatol.* **40**, 421–439 (2020).
27. Garreaud, R. D. et al. The 2010–2015 megadrought in central Chile: impacts on regional hydroclimate and vegetation. *Hydrol. Earth Syst. Sci.* **21**, 6307–6327 (2017).
28. Garreaud, R. D., Clem, K. & Veloso, J. V. The South Pacific pressure trend dipole and the Southern Blob. *J. Clim.* **34**, 7661–7676 (2021).
29. Cook, B. I., Mankin, J. S. & Anchukaitis, K. J. Climate change and drought: from past to future. *Curr. Clim. Change Rep.* **4**, 164–179 (2018).
30. Lehner, F. et al. Projected drought risk in 1.5 °C and 2 °C warmer climates. *Geophys. Res. Lett.* **44**, 7419–7428 (2017).
31. Williams, A. P. et al. Large contribution from anthropogenic warming to an emerging North American megadrought. *Science* **368**, 314–318 (2020).
32. Ault, T. R., Mankin, J. S., Cook, B. I. & Smerdon, J. E. Relative impacts of mitigation, temperature, and precipitation on 21st-century megadrought risk in the American Southwest. *Sci. Adv.* **2**, e1600873 (2016).
33. Cook, B. I., Ault, T. R. & Smerdon, J. E. Unprecedented 21st century drought risk in the American Southwest and Central Plains. *Sci. Adv.* **1**, e1400082 (2015).
34. Cook, E. R. et al. Megadroughts in North America: placing IPCC projections of hydroclimatic change in a long-term palaeoclimate context. *J. Quat. Sci.* **25**, 48–61 (2010).
35. Cook, E. R., Seager, R., Cane, M. A. & Stahle, D. W. North American drought: reconstructions, causes, and consequences. *Earth Sci. Rev.* **81**, 93–134 (2007).
36. Cook, B. I. et al. North American megadroughts in the Common Era: reconstructions and simulations. *WIREs Clim. Change* **7**, 411–432 (2016).
37. Hodell, D. A., Brenner, M. & Curtis, J. H. Terminal Classic drought in the northern Maya lowlands inferred from multiple sediment cores in Lake Chichancanab (Mexico). *Quat. Sci. Rev.* **24**, 1413–1427 (2005).
38. Lough, J. M. Tropical river flow and rainfall reconstructions from coral luminescence: Great Barrier Reef, Australia. *Paleoceanography* **22**, PA2218 (2007).
39. Woodhouse, C. A., Meko, D. M., MacDonald, G. M., Stahle, D. W. & Cook, E. R. A 1200-year perspective of 21st century drought in southwestern North America. *Proc. Natl Acad. Sci. USA* **107**, 21283–21288 (2010).
40. Steiger, N. J. et al. Oceanic and radiative forcing of medieval megadroughts in the American Southwest. *Sci. Adv.* **5**, eaax0087 (2019).
41. Cook, E. R. et al. The European Russia Drought Atlas (1400–2016 CE). *Clim. Dyn.* **54**, 2317–2335 (2020).
42. Cook, E. R. et al. Old World megadroughts and pluvials during the Common Era. *Sci. Adv.* **1**, e1500561 (2015).
43. Cook, E. R. et al. Asian monsoon failure and megadrought during the last millennium. *Science* **328**, 486 (2010).
44. Stahle, D. W. et al. The Mexican Drought Atlas: tree-ring reconstructions of the soil moisture balance during the late pre-Hispanic, colonial, and modern eras. *Quat. Sci. Rev.* **149**, 34–60 (2016).
45. Morales, M. S. et al. Six hundred years of South American tree rings reveal an increase in severe hydroclimatic events since mid-20th century. *Proc. Natl Acad. Sci. USA* **117**, 16816–16823 (2020).
46. Palmer, J. G. et al. Drought variability in the eastern Australia and New Zealand summer drought atlas (ANZDA, CE 1500–2012) modulated by the Interdecadal Pacific Oscillation. *Environ. Res. Lett.* **10**, 124002 (2015).
47. Marvel, K. et al. Twentieth-century hydroclimate changes consistent with human influence. *Nature* **569**, 59–65 (2019).
48. Anchukaitis, K. J. et al. Coupled modes of North Atlantic Ocean–atmosphere variability and the onset of the Little Ice Age. *Geophys. Res. Lett.* **46**, 12417–12426 (2019).
49. Baek, S. H. et al. Precipitation, temperature, and teleconnection signals across the combined North American, Monsoon Asia, and Old World Drought Atlases. *J. Clim.* **30**, 7141–7155 (2017).
50. Williams, A. P. et al. Tree rings and observations suggest no stable cycles in Sierra Nevada cool-season precipitation. *Water Resour. Res.* **57**, e2020WR028599 (2021).
51. Dettinger, M. D., Ralph, F. M., Das, T., Neiman, P. J. & Cayan, D. R. Atmospheric rivers, floods and the water resources of California. *Water* **3**, 445–478 (2011).
52. Ault, T. R., Cole, J. E., Overpeck, J. T., Pederson, G. T. & Meko, D. M. Assessing the risk of persistent drought using climate model simulations and paleoclimate data. *J. Clim.* **27**, 7529–7549 (2014).
53. Ault, T. R. et al. The continuum of hydroclimate variability in western North America during the last millennium. *J. Clim.* **26**, 5863–5878 (2013).
54. Huybers, P. & Curry, W. Links between annual, Milankovitch and continuum temperature variability. *Nature* **441**, 329–332 (2006).
55. Redmond, K. T. The depiction of drought: a commentary. *Bull. Am. Meteorol. Soc.* **83**, 1143–1147 (2002).

56. Dracup, J. A., Lee, K. S. & Paulson, E. G. Jr On the definition of droughts. *Water Resour. Res.* **16**, 297–302 (1980).
57. Coats, S., Smerdon, J. E., Cook, B. I. & Seager, R. Are simulated megadroughts in the North American Southwest forced? *J. Clim.* **28**, 124–142 (2015).
58. Coats, S., Smerdon, J. E., Seager, R., Cook, B. I. & González-Rouco, J. F. Megadroughts in southwestern North America in ECHO-G millennial simulations and their comparison to proxy drought reconstructions. *J. Clim.* **26**, 7635–7649 (2013).
59. Cook, B. I. et al. Uncertainties, limits, and benefits of climate change mitigation for soil moisture drought in southwestern North America. *Earths Future* **9**, e2021EF002014 (2021).
60. Stevenson, S. et al. Climate variability, volcanic forcing, and last millennium hydroclimate extremes. *J. Clim.* **31**, 4309–4327 (2018).
61. Williams, A. P., Cook, B. I. & Smerdon, J. E. Rapid intensification of the emerging southwestern North American megadrought in 2021. *Nat. Clim. Change* **12**, 232–234 (2022).
62. Meehl, G. A. & Hu, A. Megadroughts in the Indian monsoon region and southwest North America and a mechanism for associated multidecadal Pacific Sea surface temperature anomalies. *J. Clim.* **19**, 1605–1623 (2006).
63. Herweijer, C., Seager, R., Cook, E. R. & Emile-Geay, J. North American droughts of the last millennium from a gridded network of tree-ring data. *J. Clim.* **20**, 1353–1376 (2007).
64. Douglass, A. E. The secret of the Southwest solved by talkative tree rings. *Natl Geogr.* **56**, 737–770 (1929).
65. Douglass, A. E. *Dating Pueblo Bonito and Other Ruins of the Southwest* (National Geographic Society, 1935).
66. Robeson, S. M., Maxwell, J. T. & Ficklin, D. L. Bias correction of paleoclimatic reconstructions: a new look at 1,200+ years of Upper Colorado River flow. *Geophys. Res. Lett.* **47**, e2019GL086689 (2020).
67. Stahle, D. W. et al. Tree-ring data document 16th century megadrought over North America. *EOS Trans. Am. Geophys. Union.* **81**, 121–125 (2000).
68. Cook, B. I. et al. Cold tropical Pacific sea surface temperatures during the late sixteenth-century North American megadrought. *J. Geophys. Res. Atmos.* **123**, 307–11,320 (2018).
69. Stahle, D. W., Fye, F. K., Cook, E. R. & Griffin, R. D. Tree-ring reconstructed megadroughts over North America since A.D. 1300. *Clim. Change* **83**, 133 (2007).
70. Benson, L., Petersen, K. & Stein, J. Anasazi (Pre-Columbian Native-American) migrations during the middle-12th and late-13th centuries — were they drought induced? *Clim. Change* **83**, 187–213 (2007).
71. Kohler, T. A. in *Leaving Mesa Verde: Peril and Change in the Thirteenth-century Southwest* 75–101 (Univ. of Arizona Press, 2010).
72. Benson, L. V. et al. Possible impacts of early-11th-, middle-12th-, and late-13th-century droughts on western Native Americans and the Mississippian Cahokians. *Quat. Sci. Rev.* **26**, 336–350 (2007).
73. Stahle, D. W., Cleaveland, M. K., Blanton, D. B., Therrell, M. D. & Gay, D. A. The lost colony and Jamestown droughts. *Science* **280**, 564–567 (1998).
74. Schroeder, A. H. Shifting for survival in the Spanish Southwest. *N M Hist. Rev.* **43**, 4 (1968).
75. Marlon, J. R. et al. Long-term perspective on wildfires in the western USA. *Proc. Natl Acad. Sci. USA* **109**, E535 (2012).
76. Calder, W. J., Parker, D., Stopka, C. J., Jiménez-Moreno, G. & Shuman, B. N. Medieval warming initiated exceptionally large wildfire outbreaks in the Rocky Mountains. *Proc. Natl Acad. Sci. USA* **112**, 13261 (2015).
77. Halfen, A. F. et al. Activation history of the Hutchinson dunes in east-central Kansas, USA during the past 2200 years. *Aeolian Res.* **5**, 9–20 (2012).
78. Hanson, P. R., Arbogast, A. F., Johnson, W. C., Joeckel, R. M. & Young, A. R. Megadroughts and late Holocene dune activation at the eastern margin of the Great Plains, north-central Kansas, USA. *Aeolian Res.* **1**, 101–110 (2010).
79. Forman, S. L., Oglesby, R. & Webb, R. S. Temporal and spatial patterns of Holocene dune activity on the Great Plains of North America: megadroughts and climate links. *Glob. Planet. Change* **29**, 1–29 (2001).
80. Miao, X. et al. A 10,000 year record of dune activity, dust storms, and severe drought in the central Great Plains. *Geology* **35**, 119–122 (2007).
81. Hodell, D. A., Curtis, J. H. & Brenner, M. Possible role of climate in the collapse of Classic Maya civilization. *Nature* **375**, 391–394 (1995).
82. Hodell, D. A., Brenner, M., Curtis, J. H. & Guilderson, T. Solar forcing of drought frequency in the Maya lowlands. *Science* **292**, 1367–1370 (2001).
83. Douglas, P. M. J. et al. Drought, agricultural adaptation, and sociopolitical collapse in the Maya lowlands. *Proc. Natl Acad. Sci.USA* **112**, 5607 (2015).
84. Curtis, J. H., Hodell, D. A. & Brenner, M. Climate variability on the Yucatan Peninsula (Mexico) during the past 3500 years, and implications for Maya cultural evolution. *Quat. Res.* **46**, 37–47 (1996).
85. Medina-Elizalde, M. et al. High resolution stalagmite climate record from the Yucatán Peninsula spanning the Maya terminal classic period. *Earth Planet. Sci. Lett.* **298**, 255–262 (2010).
86. Haug, G. H. et al. Climate and the collapse of Maya civilization. *Science* **299**, 1731–1735 (2003).
87. Medina-Elizalde, M. & Rohling, E. J. Collapse of classic Maya civilization related to modest reduction in precipitation. *Science* **335**, 956–959 (2012).
88. Evans, N. P. et al. Quantification of drought during the collapse of the classic Maya civilization. *Science* **361**, 498–501 (2018).
89. Aimers, J. & Hodell, D. Drought and the Maya. *Nature* **479**, 44–45 (2011).
90. Gioda, A. & del R.Prieto, M. Histoire des sécheresses Andines; Potosi, El Niño et le petit âge glaciaire. *La Météorologie* **27**, 33–42 (1999).
91. Bird, B. W. et al. A 2,300-year-long annually resolved record of the South American summer monsoon from the Peruvian Andes. *Proc. Natl Acad. Sci. USA* **108**, 8583–8588 (2011).
92. Granato-Souza, D. et al. Multidecadal changes in wet season precipitation totals over the eastern Amazon. *Geophys. Res. Lett.* **47**, e2020GL087478 (2020).
93. Touchan, R. et al. Spatiotemporal drought variability in northwestern Africa over the last nine centuries. *Clim. Dyn.* **37**, 237–252 (2011).
94. Nash, D. J. et al. African hydroclimatic variability during the last 2000 years. *Quat. Sci. Rev.* **154**, 1–22 (2016).
95. Tierney, J. E., Smerdon, J. E., Anchukaitis, K. J. & Seager, R. Multidecadal variability in East African hydroclimate controlled by the Indian Ocean. *Nature* **493**, 389–392 (2013).
96. Anchukaitis, K. J. & Tierney, J. E. Identifying coherent spatiotemporal modes in time-uncertain proxy paleoclimate records. *Clim. Dyn.* **41**, 1291–1306 (2013).
97. Halfman, J. D., Johnson, T. C. & Finney, B. P. New AMS dates, stratigraphic correlations and decadal climatic cycles for the past 4 ka at Lake Turkana, Kenya. *Palaeogeogr. Palaeoclimatol. Palaeoecol.* **111**, 83–98 (1994).
98. Buckles, L. K. et al. Interannual and (multi-)decadal variability in the sedimentary BIT index of Lake Challa, East Africa, over the past 2200 years: assessment of the precipitation proxy. *Clim. Past.* **12**, 1243–1262 (2016).
99. Russell, J. M. & Johnson, T. C. A high-resolution geochemical record from Lake Edward, Uganda Congo and the timing and causes of tropical African drought during the late Holocene. *Quat. Sci. Rev.* **24**, 1375–1389 (2005).
100. Russell, J. M. & Johnson, T. C. Little Ice Age drought in equatorial Africa: intertropical convergence zone migrations and El Niño-Southern Oscillation variability. *Geology* **35**, 21–24 (2007).
101. Owen, R. B. et al. Major low levels of Lake Malawi and their implications for speciation rates in cichlid fishes. *Proc. R. Soc. B: Biol. Sci.* **240**, 519–553 (1990).
102. Nicholson, S. E. Historical and modern fluctuations of Lakes Tanganyika and Rukwa and their relationship to rainfall variability. *Clim. Change* **41**, 53–71 (1999).
103. Nicholson, S. E., Klotter, D. & Dezfuli, A. K. Spatial reconstruction of semi-quantitative precipitation fields over Africa during the nineteenth century from documentary evidence and gauge data. *Quat. Res.* **78**, 13–23 (2012).
104. Stager, J. C., Ryves, D., Cumming, B. F., Meeker, L. D. & Beer, J. Solar variability and the levels of Lake Victoria, East Africa, during the last millenium. *J. Paleolimnol.* **33**, 243–251 (2005).
105. Kiage, L. M. & Liu, K. Palynological evidence of climate change and land degradation in the Lake Baringo area, Kenya, East Africa, since AD 1650. *Palaeogeogr. Palaeoclimatol. Palaeoecol.* **279**, 60–72 (2009).
106. Legesse, D. et al. Environmental changes in a tropical lake (Lake Abiyata, Ethiopia) during recent centuries. *Palaeogeogr. Palaeoclimatol. Palaeoecol.* **187**, 233–258 (2002).
107. Wils, T. H. G. et al. Towards a reconstruction of Blue Nile baseflow from Ethiopian tree rings. *Holocene* **20**, 837–848 (2010).
108. Pankhurst, R. The Great Ethiopian Famine of 1888–1892: a new assessment. *J. History Med. Allied Sci.* **XXI**, 95–124 (1966).
109. Miller, J. C. The significance of drought, disease and famine in the agriculturally marginal zones of west-central Africa. *J. Afr. History* **23**, 17–61 (1982).
110. Ngomanda, A. et al. Lowland rainforest response to hydrological changes during the last 1500 years in Gabon, Western Equatorial Africa. *Quat. Res.* **67**, 411–425 (2007).
111. Verschuren, D. in *Past Climate Variability through Europe and Africa* (eds Battarbee, R. W., Gasse, F. & Stickley, C. E.) 139–158 (Springer Netherlands, 2004).
112. Shanahan, T. M. et al. Atlantic forcing of persistent drought in West Africa. *Science* **324**, 377–380 (2009).
113. Nguetsop, V. F., Servant-Vildary, S., Servant, M. & Roux, M. Long and short-time scale climatic variability in the last 5500 years in Africa according to modern and fossil diatoms from Lake Ossa (western Cameroon). *Glob. Planet. Change* **72**, 356–367 (2010).
114. Norrgård, S. Practising historical climatology in West Africa: a climatic periodisation 1750–1800. *Clim. Change* **129**, 131–143 (2015).
115. Büntgen, U. et al. Recent European drought extremes beyond Common Era background variability. *Nat. Geosci.* **14**, 190–196 (2021).
116. Büntgen, U. et al. 2500 years of European climate variability and human susceptibility. *Science* **331**, 578–582 (2011).
117. Nicault, A. et al. Mediterranean drought fluctuation during the last 500 years based on tree-ring data. *Clim. Dyn.* **31**, 227–245 (2008).
118. Gorostiza, S., Martí Escayol, M. A. & Barriendos, M. Controlling water infrastructure and codifying water knowledge: institutional responses to severe drought in Barcelona (1620–1650). *Clim. Past.* **17**, 913–927 (2021).
119. Oliva, M. et al. The Little Ice Age in Iberian mountains. *Earth Sci. Rev.* **177**, 175–208 (2018).
120. Sinha, A. et al. A global context for megadroughts in monsoon Asia during the past millennium. *Quat. Sci. Rev.* **30**, 47–62 (2011).
121. Sinha, A. et al. A 900-year (600 to 1500 A.D.) record of the Indian summer monsoon precipitation from the core monsoon zone of India. *Geophys. Res. Lett.* https://doi.org/10.1029/2007GL030431 (2007).
122. Buckley, B. M. et al. Climate as a contributing factor in the demise of Angkor, Cambodia. *Proc. Natl Acad. Sci. USA* **107**, 6748–6752 (2010).
123. Zhang, X., Bai, M., Hao, Z. & Zheng, J. Potential causes of megadroughts in North China in the preindustrial period from the teleconnection perspective. *Glob. Planet. Change* **205**, 103596 (2021).
124. Zheng, J. et al. How climate change impacted the collapse of the Ming dynasty. *Clim. Change* **127**, 169–182 (2014).
125. Singh, D. et al. Climate and the global famine of 1876–78. *J. Clim.* **31**, 9445–9467 (2018).
126. Mishra, V. et al. Drought and famine in India, 1870–2016. *Geophys. Res. Lett.* **46**, 2075–2083 (2019).
127. Davis, M. *Late Victorian Holocausts: El Niño Famines and the Making of the Third World* (Verso, 2002).
128. van Ommen, T. D. & Morgan, V. Snowfall increase in coastal East Antarctica linked with southwest Western Australian drought. *Nat. Geosci.* **3**, 267–272 (2010).
129. Tozer, C. R. et al. An ice core derived 1013-year catchment-scale annual rainfall reconstruction in subtropical eastern Australia. *Hydrol. Earth Syst. Sci.* **20**, 1703–1717 (2016).
130. Kiem, A. S. et al. Learning from the past — using palaeoclimate data to better understand and manage drought in South East Queensland (SEQ), Australia. *J. Hydrol. Reg. Stud.* **29**, 100686 (2020).
131. Ho, M., Kiem, A. S. & Verdon-Kidd, D. C. A paleoclimate rainfall reconstruction in the Murray-Darling Basin (MDB), Australia: 2. Assessing hydroclimatic risk using paleoclimate records of wet and dry epochs. *Water Resour. Res.* **51**, 8380–8396 (2015).
132. Cook, B. I. et al. The paleoclimate context and future trajectory of extreme summer hydroclimate in eastern Australia. *J. Geophys. Res. Atmos.* **121**, 12820–12838 (2016).

133. Cullen, L. E. & Grierson, P. F. Multi-decadal scale variability in autumn–winter rainfall in south-western Australia since 1655 AD as reconstructed from tree rings of *Callitris columellaris*. *Clim. Dyn.* **33**, 433–444 (2009).
134. Gallant, A. J. E. & Gergis, J. An experimental streamflow reconstruction for the River Murray, Australia, 1783–1988. *Water Resour. Res.* **47**, W00G04 (2011).
135. Allen, K. J. et al. Preliminary December–January inflow and streamflow reconstructions from tree rings for western Tasmania, southeastern Australia. *Water Resour. Res.* **51**, 5487–5503 (2015).
136. Vance, T. R., van Ommen, T. D., Curran, M. A. J., Plummer, C. T. & Moy, A. D. A millennial proxy record of ENSO and eastern Australian rainfall from the Law Dome Ice Core, East Antarctica. *J. Clim.* **26**, 710–725 (2013).
137. Bai, M., Zheng, J., Hao, Z., Zhang, X. & Zeng, G. Hydroclimate patterns over the northern hemisphere when megadroughts occurred in North China during the last millennium. *Clim. Change* **157**, 365–385 (2019).
138. Jungclaus, J. H. et al. The PMIP4 contribution to CMIP6 — part 3: the last millennium, scientific objective, and experimental design for the PMIP4 past1000 simulations. *Geosci. Model. Dev.* **10**, 4005–4033 (2017).
139. Stevenson, S., Otto-Bliesner, B., Fasullo, J. & Brady, E. "El Niño Like" hydroclimate responses to last millennium volcanic eruptions. *J. Clim.* **29**, 2907–2921 (2016).
140. Seager, R. et al. Blueprints for medieval hydroclimate. *Quat. Sci. Rev.* **26**, 2322–2336 (2007).
141. Clement, A. C., Seager, R., Cane, M. A. & Zebiak, S. E. An ocean dynamical thermostat. *J. Clim.* **9**, 2190–2196 (1996).
142. Coats, S., Smerdon, J. E., Karnauskas, K. B. & Seager, R. The improbable but unexceptional occurrence of megadrought clustering in the American West during the Medieval Climate Anomaly. *Environ. Res. Lett.* **11**, 074025 (2016).
143. Ault, T. R. et al. A robust null hypothesis for the potential causes of megadrought in western North America. *J. Clim.* **31**, 3–24 (2018).
144. Tejedor, E., Steiger, N. J., Smerdon, J. E., Serrano-Notivoli, R. & Vuille, M. Global hydroclimatic response to tropical volcanic eruptions over the last millennium. *Proc. Natl Acad. Sci. USA* **118**, e2019145118 (2021).
145. Rao, M. P. et al. European and Mediterranean hydroclimate responses to tropical volcanic forcing over the last millennium. *Geophys. Res. Lett.* **44**, 5104–5112 (2017).
146. Kim, W. M. & Raible, C. C. Dynamics of the Mediterranean droughts from 850 to 2099 CE in the Community Earth System Model. *Clim. Past.* **17**, 887–911 (2021).
147. Anchukaitis, K. J. et al. Influence of volcanic eruptions on the climate of the Asian monsoon region. *Geophys. Res. Lett.* https://doi.org/10.1029/2010GL044843 (2010).
148. Stevenson, S., Timmermann, A., Chikamoto, Y., Langford, S. & DiNezio, P. Stochastically generated North American megadroughts. *J. Clim.* **28**, 1865–1880 (2015).
149. Coats, S. et al. Internal ocean–atmosphere variability drives megadroughts in western North America. *Geophys. Res. Lett.* **43**, 9886–9894 (2016).
150. Hunt, B. G. Global characteristics of pluvial and dry multi-year episodes, with emphasis on megadroughts. *Int. J. Climatol.* **31**, 1425–1439 (2011).
151. Trenberth, K. E. et al. Progress during TOGA in understanding and modeling global teleconnections associated with tropical sea surface temperatures. *J. Geophys. Res. Ocean.* **103**, 14291–14324 (1998).
152. Feng, S., Oglesby, R. J., Rowe, C. M., Loope, D. B. & Hu, Q. Atlantic and Pacific SST influences on medieval drought in North America simulated by the community atmospheric model. *Journal of Geophysical Research: Atmospheres* https://doi.org/10.1029/2007JD009347 (2008).
153. Seager, R. et al. Tropical Pacific forcing of North American medieval megadroughts: testing the concept with an atmosphere model forced by coral-reconstructed SSTs. *J. Clim.* **21**, 6175–6190 (2008).
154. Seager, R. et al. Mechanisms of ENSO-forcing of hemispherically symmetric precipitation variability. *Q. J. R. Meteorol. Soc.* **131**, 1501–1527 (2005).
155. Seager, R., Harnik, N., Kushnir, Y., Robinson, W. & Miller, J. Mechanisms of hemispherically symmetric climate variability. *J. Clim.* **16**, 2960–2978 (2003).
156. Ning, L. et al. Variability and mechanisms of megadroughts over eastern China during the last millennium: a model study. *Atmosphere* **10**, 7 (2019).
157. Wu, H. C. et al. Changes to Yucatán Peninsula precipitation associated with salinity and temperature extremes of the Caribbean Sea during the Maya civilization collapse. *Sci. Rep.* **7**, 15825 (2017).
158. Ummenhofer, C. C., D'Arrigo, R. D., Anchukaitis, K. J., Buckley, B. M. & Cook, E. R. Links between Indo-Pacific climate variability and drought in the Monsoon Asia Drought Atlas. *Clim. Dyn.* **40**, 1319–1334 (2013).
159. Seager, R. et al. Strengthening tropical Pacific zonal sea surface temperature gradient consistent with rising greenhouse gases. *Nat. Clim. Change* **9**, 517–522 (2019).
160. Delworth, T. L., Zeng, F., Rosati, A., Vecchi, G. A. & Wittenberg, A. T. A link between the hiatus in global warming and North American drought. *J. Clim.* **28**, 3834–3845 (2015).
161. Seneviratne, S. I. et al. Investigating soil moisture–climate interactions in a changing climate: a review. *Earth Sci. Rev.* **99**, 125–161 (2010).
162. Zhou, S. et al. Land–atmosphere feedbacks exacerbate concurrent soil drought and atmospheric aridity. *Proc. Natl Acad. Sci. USA* **116**, 18848 (2019).
163. Zhou, S. et al. Soil moisture–atmosphere feedbacks mitigate declining water availability in drylands. *Nat. Clim. Change* **11**, 38–44 (2021).
164. Tierney, J. E., Pausata, F. S. R. & deMenocal, P. B. Rainfall regimes of the Green Sahara. *Sci. Adv.* **3**, e1601503 (2021).
165. Guo, Z. et al. GLACE: the global land–atmosphere coupling experiment. Part II: analysis. *J. Hydrometeorol.* **7**, 611–625 (2006).
166. Cook, B. I., Miller, R. L. & Seager, R. Amplification of the North American "Dust Bowl" drought through human-induced land degradation. *Proc. Natl Acad. Sci. USA* **106**, 4997 (2009).
167. Giannini, A., Saravanan, R. & Chang, P. Oceanic forcing of Sahel rainfall on interannual to interdecadal time scales. *Science* **302**, 1027–1030 (2003).
168. Cook, B. I., Seager, R., Miller, R. L. & Mason, J. A. Intensification of North American megadroughts through surface and dust aerosol forcing. *J. Clim.* **26**, 4414–4430 (2013).
169. Cook, B. I. et al. Pre-Columbian deforestation as an amplifier of drought in Mesoamerica. *Geophys. Res. Lett.* **39**, 16706 (2012).
170. Oglesby, R. J., Sever, T. L., Saturno, W., Erickson, D. J. III & Srikishen, J. Collapse of the Maya: could deforestation have contributed? *J. Geophys. Res. Atmos.* https://doi.org/10.1029/2009JD011942 (2010).
171. Marvel, K. et al. Observed and projected changes to the precipitation annual cycle. *J. Clim.* **30**, 4983–4995 (2017).
172. Marvel, K. & Bonfils, C. Identifying external influences on global precipitation. *Proc. Natl Acad. Sci.* **110**, 19301–19306 (2013).
173. Hoerling, M. et al. On the increased frequency of Mediterranean drought. *J. Clim.* **25**, 2146–2161 (2012).
174. Siirila-Woodburn, E. R. et al. A low-to-no snow future and its impacts on water resources in the western United States. *Nat. Rev. Earth Environ.* https://doi.org/10.1038/s43017-021-00219-y (2021).
175. Mote, P. W., Li, S., Lettenmaier, D. P., Xiao, M. & Engel, R. Dramatic declines in snowpack in the western US. *npj Clim. Atmos. Sci.* **1**, 2 (2018).
176. Liu, J. et al. Contributions of anthropogenic forcings to evapotranspiration changes over 1980–2020 using GLEAM and CMIP6 simulations. *J. Geophys. Res. Atmos.* **126**, e2021JD035367 (2021).
177. Wang, R. et al. Recent increase in the observation-derived land evapotranspiration due to global warming. *Environ. Res. Lett.* **17**, 24020 (2022).
178. Mankin, J. S. et al. *NOAA Drought Task Force Report on the 2020–2021 Southwestern US Drought* (NOAA Drought Task Force, MAPP, and NIDIS, 2021).
179. Zhuang, Y., Fu, R., Santer, B. D., Dickinson, R. E. & Hall, A. Quantifying contributions of natural variability and anthropogenic forcings on increased fire weather risk over the western United States. *Proc. Natl Acad. Sci. USA* **118**, e2111875118 (2021).
180. McVicar, T. R. et al. Global review and synthesis of trends in observed terrestrial near-surface wind speeds: implications for evaporation. *J. Hydrol.* **416–417**, 182–205 (2012).
181. Swann, A. L. S. Plants and drought in a changing climate. *Curr. Clim. Change Rep.* **4**, 192–201 (2018).
182. Mankin, J. S., Seager, R., Smerdon, J. E., Cook, B. I. & Williams, A. P. Mid-latitude freshwater availability reduced by projected vegetation responses to climate change. *Nat. Geosci.* **12**, 983–988 (2019).
183. Mankin, J. S. et al. Blue water trade-offs with vegetation in a CO_2-enriched climate. *Geophys. Res. Lett.* **45**, 3115–3125 (2018).
184. Griffin, D. & Anchukaitis, K. J. How unusual is the 2012–2014 California drought? *Geophys. Res. Lett.* **41**, 9017–9023 (2014).
185. Williams, A. P. et al. Contribution of anthropogenic warming to California drought during 2012–2014. *Geophys. Res. Lett.* **42**, 6819–6828 (2015).
186. Woodhouse, C. A., Pederson, G. T., Morino, K., McAfee, S. A. & McCabe, G. J. Increasing influence of air temperature on upper Colorado River streamflow. *Geophys. Res. Lett.* **43**, 2174–2181 (2016).
187. Berg, N. & Hall, A. Anthropogenic warming impacts on California snowpack during drought. *Geophys. Res. Lett.* **44**, 2511–2518 (2017).
188. Xiao, M., Udall, B. & Lettenmaier, D. P. On the causes of declining Colorado River streamflows. *Water Resour. Res.* **54**, 6739–6756 (2018).
189. Harley, G. L., Maxwell, R. S., Black, B. A. & Bekker, M. F. A multi-century, tree-ring-derived perspective of the North Cascades (USA) 2014–2016 snow drought. *Clim. Change* **162**, 127–143 (2020).
190. Huang, X., Hall, A. D. & Berg, N. Anthropogenic warming impacts on today's Sierra Nevada snowpack and flood risk. *Geophys. Res. Lett.* **45**, 6215–6222 (2018).
191. Mote, P. W. et al. Perspectives on the causes of exceptionally low 2015 snowpack in the western United States. *Geophys. Res. Lett.* **43**, 10980–10988 (2016).
192. Huning, L. S. & AghaKouchak, A. Global snow drought hot spots and characteristics. *Proc. Natl Acad. Sci. USA* **117**, 19753–19759 (2020).
193. Seager, R. et al. Climate variability and change of Mediterranean-type climates. *J. Clim.* **32**, 2887–2915 (2019).
194. Gudmundsson, L. & Seneviratne, S. I. Anthropogenic climate change affects meteorological drought risk in Europe. *Environ. Res. Lett.* **11**, 044005 (2016).
195. Kelley, C. P., Mohtadi, S., Cane, M. A., Seager, R. & Kushnir, Y. Climate change in the Fertile Crescent and implications of the recent Syrian drought. *Proc. Natl Acad. Sci. USA* **112**, 3241 (2015).
196. Pascale, S., Kapnick, S. B., Delworth, T. L., Hidalgo, H. G. & Cooke, W. F. Natural variability vs forced signal in the 2015–2019 Central American drought. *Clim. Change* **168**, 16 (2021).
197. Herrera, D. A. et al. Exacerbation of the 2013–2016 pan-Caribbean drought by anthropogenic warming. *Geophys. Res. Lett.* **45**, 10619–10626 (2018).
198. Pascale, S., Kapnick, S. B., Delworth, T. L. & Cooke, W. F. Increasing risk of another Cape Town "Day Zero" drought in the 21st century. *Proc. Natl Acad. Sci. USA* **117**, 29495 (2020).
199. Otto, F. E. L. et al. Anthropogenic influence on the drivers of the Western Cape drought 2015–2017. *Environ. Res. Lett.* **13**, 124010 (2018).
200. Delworth, T. L. & Zeng, F. Regional rainfall decline in Australia attributed to anthropogenic greenhouse gases and ozone levels. *Nat. Geosci.* **7**, 583–587 (2014).
201. Overpeck, J. T. & Udall, B. Climate change and the aridification of North America. *Proc. Natl Acad. Sci. USA* **117**, 11856 (2020).
202. Jasechko, S. & Perrone, D. California's central valley groundwater wells run dry during recent drought. *Earths Future* **8**, e2019EF001339 (2020).
203. Cooley, H., Donnelly, K., Phurisamban, R. & Subramanian, M. *Impacts of California's Ongoing Drought: Agriculture* Vol. 24 (Pacific Institute, 2015).
204. Williams, A. P. et al. Observed impacts of anthropogenic climate change on wildfire in California. *Earths Future* **7**, 892–910 (2019).
205. Abatzoglou, J. T. & Williams, A. P. Impact of anthropogenic climate change on wildfire across western US forests. *Proc. Natl Acad. Sci. USA* **113**, 11770 (2016).
206. Lehner, F., Deser, C., Simpson, I. R. & Terray, L. Attributing the US Southwest's recent shift into drier conditions. *Geophys. Res. Lett.* **45**, 6251–6261 (2018).
207. Seager, R. et al. Causes of the 2011–14 California drought. *J. Clim.* **28**, 6997–7024 (2015).

208. Ficklin, D. L. & Novick, K. A. Historic and projected changes in vapor pressure deficit suggest a continental-scale drying of the United States atmosphere. *J. Geophys. Res. Atmos.* **122**, 2061–2079 (2017).
209. Chiodi, A. M., Potter, B. E. & Larkin, N. K. Multi-decadal change in western US nighttime vapor pressure deficit. *Geophys. Res. Lett.* **48**, e2021GL092830 (2021).
210. Seager, R. et al. Climatology, variability, and trends in the US vapor pressure deficit, an important fire-related meteorological quantity. *J. Appl. Meteorol. Climatol.* **54**, 1121–1141 (2015).
211. Muñoz, A. A. et al. Water crisis in Petorca Basin, Chile: the combined effects of a mega-drought and water management. *Water* **12**, 648 (2020).
212. Serrano-Notivoli, R. et al. Hydroclimatic variability in Santiago (Chile) since the 16th century. *Int. J. Climatol.* **41**, E2015–E2030 (2021).
213. Boisier, J. P., Rondanelli, R., Garreaud, R. D. & Muñoz, F. Anthropogenic and natural contributions to the Southeast Pacific precipitation decline and recent megadrought in central Chile. *Geophys. Res. Lett.* **43**, 413–421 (2016).
214. Fuentealba, M., Bahamóndez, C., Sarricolea, P., Meseguer-Ruiz, O. & Latorre, C. The 2010–2020 "megadrought" drives reduction in lake surface area in the Andes of central Chile (32°–36° S). *J. Hydrol. Reg. Stud.* **38**, 100952 (2021).
215. Alvarez-Garreton, C., Boisier, J. P., Garreaud, R., Seibert, J. & Vis, M. Progressive water deficits during multiyear droughts in basins with long hydrological memory in Chile. *Hydrol. Earth Syst. Sci.* **25**, 429–446 (2021).
216. Shaw, T. E. et al. Glacier albedo reduction and drought effects in the extratropical Andes, 1986–2020. *J. Glaciol.* **67**, 158–169 (2021).
217. Rivera, J. A., Otta, S., Lauro, C. & Zazulie, N. A decade of hydrological drought in central-western Argentina. *Front. Water* https://doi.org/10.3389/frwa.2021.640544 (2021).
218. González, M. E., Gómez-González, S., Lara, A., Garreaud, R. & Díaz-Hormazábal, I. The 2010–2015 megadrought and its influence on the fire regime in central and south-central Chile. *Ecosphere* **9**, e02300 (2018).
219. Zappa, G. Regional climate impacts of future changes in the mid-latitude atmospheric circulation: a storyline view. *Curr. Clim. Change Rep.* **5**, 358–371 (2019).
220. Boisier, J. P. et al. Anthropogenic drying in central-southern Chile evidenced by long-term observations and climate model simulations. *Elementa* **6**, 74 (2018).
221. Seneviratne, S. I. et al. in *Climate Change 2021: The Physical Science Basis. Contribution of Working Group I to the Sixth Assessment Report of the Intergovernmental Panel on Climate Change* (eds Zhao, B. et al.) 1513–1766 (Cambridge Univ. Press, 2021).
222. Cook, B. I. et al. Twenty-first century drought projections in the CMIP6 forcing scenarios. *Earths Future* **8**, e2019EF001461 (2020).
223. Ukkola, A. M., de Kauwe, M. G., Roderick, M. L., Abramowitz, G. & Pitman, A. J. Robust future changes in meteorological drought in CMIP6 projections despite uncertainty in precipitation. *Geophys. Res. Lett.* **47**, e2020GL087820 (2020).
224. Mankin, J. S., Viviroli, D., Singh, D., Hoekstra, A. Y. & Diffenbaugh, N. S. The potential for snow to supply human water demand in the present and future. *Environ. Res. Lett.* **10**, 114016 (2015).
225. Livneh, B. & Badger, A. M. Drought less predictable under declining future snowpack. *Nat. Clim. Change* **10**, 452–458 (2020).
226. Vicente-Serrano, S. M., McVicar, T. R., Miralles, D. G., Yang, Y. & Tomas-Burguera, M. Unraveling the influence of atmospheric evaporative demand on drought and its response to climate change. *WIREs Clim. Change* **11**, e632 (2020).
227. Tuel, A., O'Gorman, P. A. & Eltahir, E. A. B. Elements of the dynamical response to climate change over the Mediterranean. *J. Clim.* **34**, 1135–1146 (2021).
228. Stevenson, S. et al. Twenty-first century hydroclimate: a continually changing baseline, with more frequent extremes. *Proc. Natl Acad. Sci. USA* **119**, e2108124119 (2022).
229. Mankin, J. S., Lehner, F., Coats, S. & McKinnon, K. A. The value of initial condition large ensembles to robust adaptation decision-making. *Earths Future* **8**, e2012EF001610 (2020).
230. Coats, S. & Mankin, J. S. The challenge of accurately quantifying future megadrought risk in the American Southwest. *Geophys. Res. Lett.* **43**, 9225–9233 (2016).
231. Field, J. P. et al. Forest management under megadrought: urgent needs at finer scale and higher intensity. *Front. For. Glob. Change* **3**, 140 (2020).
232. Coats, S. et al. Paleoclimate constraints on the spatiotemporal character of past and future droughts. *J. Clim.* **33**, 9883–9903 (2020).
233. Huang, X. & Stevenson, S. Connections between mean North Pacific circulation and western US precipitation extremes in a warming climate. *Earths Future* **9**, e2020EF001944 (2021).
234. Chiang, F., Mazdiyasni, O. & AghaKouchak, A. Amplified warming of droughts in southern United States in observations and model simulations. *Sci. Adv.* **4**, eaat2380 (2021).
235. Hessl, A. E. et al. Past and future drought in Mongolia. *Sci. Adv.* **4**, e1701832 (2021).
236. Parsons, L. A. Implications of CMIP6 projected drying trends for 21st century Amazonian drought risk. *Earths Future* **8**, e2020EF001608 (2020).
237. Milly, P. C. D. & Dunne, K. A. Colorado River flow dwindles as warming-driven loss of reflective snow energizes evaporation. *Science* **367**, 1252–1255 (2020).
238. Lehner, F., Wahl, E. R., Wood, A. W., Blatchford, D. B. & Llewellyn, D. Assessing recent declines in Upper Rio Grande runoff efficiency from a paleoclimate perspective. *Geophys. Res. Lett.* **44**, 4124–4133 (2017).
239. Udall, B. & Overpeck, J. The twenty-first century Colorado River hot drought and implications for the future. *Water Resour. Res.* **53**, 2404–2418 (2017).
240. van Dijk, A. I. J. M. et al. The millennium drought in southeast Australia (2001–2009): natural and human causes and implications for water resources, ecosystems, economy, and society. *Water Resour. Res.* **49**, 1040–1057 (2013).
241. Marchin, R. M. et al. Extreme heat increases stomatal conductance and drought-induced mortality risk in vulnerable plant species. *Glob. Change Biol.* **28**, 1133–1146 (2021).
242. Lehner, F. et al. The potential to reduce uncertainty in regional runoff projections from climate models. *Nat. Clim. Change* **9**, 926–933 (2019).
243. Faunt, C. C., Sneed, M., Traum, J. & Brandt, J. T. Water availability and land subsidence in the Central Valley, California, USA. *Hydrogeol. J.* **24**, 675–684 (2016).
244. Chang, J. et al. Reservoir operations to mitigate drought effects with a hedging policy triggered by the drought prevention limiting water level. *Water Resour. Res.* **55**, 904–922 (2019).
245. Apurv, T. & Cai, X. Impact of droughts on water supply in US watersheds: the role of renewable surface and groundwater resources. *Earths Future* **8**, e2020EF001648 (2020).
246. Lu, J., Carbone, G. J., Huang, X., Lackstrom, K. & Gao, P. Mapping the sensitivity of agriculture to drought and estimating the effect of irrigation in the United States, 1950–2016. *Agric. For. Meteorol.* **292–293**, 108124 (2020).
247. Pauloo, R. A. et al. Domestic well vulnerability to drought duration and unsustainable groundwater management in California's Central Valley. *Environ. Res. Lett.* **15**, 44010 (2020).
248. Kuhn, E. & Fleck, J. *Science Be Dammed: How Ignoring Inconvenient Science Drained the Colorado River* (Univ. of Arizona Press, 2019).
249. Fleck, J. & Castle, A. Green light for adaptive policies on the Colorado River. *Water* **14**, 2 (2022).
250. Grafton, R. Q. et al. The paradox of irrigation efficiency. *Science* **361**, 748–750 (2018).
251. di Baldassarre, G. et al. Water shortages worsened by reservoir effects. *Nat. Sustain.* **1**, 617–622 (2018).
252. Nielsen-Gammon, J. W. The 2011 Texas drought. *Tex. Water J.* **3**, 59–95 (2012).
253. Mix, K., Groeger, A. W. & Lopes, V. L. Impacts of dam construction on streamflows during drought periods in the Upper Colorado River Basin, Texas. *Lake Reserv. Res. Manag.* **21**, 329–337 (2016).
254. Tedesco, J. 1950s drought plagued Texas for seven long years. *San Antonio Express-News* (11 September 2015); https://www.expressnews.com/150years/major-stories/article/1950s-drought-plagued-Texas-for-seven-long-years-6500014.php.
255. Woodhouse, C. A. et al. Upper Colorado river basin 20th century droughts under 21st century warming: plausible scenarios for the future. *Clim. Serv.* **21**, 100206 (2021).
256. Verdon-Kidd, D., Beatty, R. & Allen, K. Planning urban water system responses to megadrought. *Water e-J.* **4**, 1–11 (2019).
257. Barichivich, J., Osborn, T., Harris, I., van der Schrier, G. & Jones, P. Monitoring global drought using the self-calibrating Palmer Drought Severity Index [in 'State of the Climate in 2020' eds. Dunn RJH, Aldred F, Gobron N, Miller JB & Willett KM]. *Bull. Am. Meteorol. Soc.* **102**, S68–S70 (2021).
258. Nguyen, H. T. T., Turner, S. W. D., Buckley, B. M. & Galelli, S. Coherent streamflow variability in monsoon asia over the past eight centuries — links to oceanic drivers. *Water Resour. Res.* **56**, e2020WR027883 (2020).

Acknowledgements
B.I.C., A.P.W. and K.M. are supported by National Oceanic and Atmospheric Administration (NOAA) MAPP NA19OAR4310278. B.I.C. and A.P.W. are also supported by NASA's Modeling, Analysis, and Prediction programme (MAP-16-0081). J.E.S. is supported by National Science Foundation (NSF) AGS-1805490. B.I.C., A.P.W., K.M., J.E.S., J.S.M. and R.S. are supported by Department of Energy (DOE) Grant ESC0022302. J.E.S. and R.S. are supported by NSF AGS 2101214 and R.S. is supported by NSF AGS 2127684. K.A. is supported by Australian Research Council (ARC) Grant FT200100102. L.A.-H., A.P.W. and J.E.S. are supported by NSF OISE-1743738; L.A.-H. and A.P.W. also supported by AGS-1702789 and AGS-1903687. J.E.S., R.S. and J.S.M. are supported by NOAA MAPP NA20OAR4310425. M.I. is supported by the Helmholtz Association through the joint programme 'Changing Earth — Sustaining our Future' (PoF IV) of the Alfred-Wegener-Institut and the Helmholtz Climate Initiative REKLIM. F.L. is supported by the US DOE Office of Science, Office of Biological & Environmental Research (BER), Regional and Global Model Analysis (RGMA) component of the Earth and Environmental System Modeling Program under Award Number DE-SC0022070 and NSF IA 1947282. This work was also supported by the National Center for Atmospheric Research (NCAR), which is a major facility sponsored by the NSF under Cooperative Agreement No. 1852977. M.S.M. is supported by FONDECYT-BM-INC.INV 039-2019. H.T.T.N. is supported by the Lamont-Doherty Postdoctoral Fellowship. M.P.R. and U.K.T. supported by NOAA Climate & Global Change Fellowship #NA18NWS4620043B. M.R. is supported by NASA 80NSSC21K1713. D.G. is supported by NSF-AGS 1903504. K.J.A. is supported by NSF AGS-1501856, BCS-1759629 and AGS-1803995.

Author contributions
B.I.C., J.E.S., E.R.C., A.P.W., K.J.A. and J.S.M. led the review. H.T.T.N provided Box 2 text and figure. J.S.M. provided Fig. 4. All authors contributed to the manuscript preparation, interpretation, discussion and writing.

Competing interests
The authors declare no competing interests.

Peer review information
Nature Reviews Earth & Environment thanks Brad Udall, Eduardo Zorita and Matteo Zampieri for their contribution to the peer review of this work.

Publisher's note
Springer Nature remains neutral with regard to jurisdictional claims in published maps and institutional affiliations.

Supplementary information
The online version contains supplementary material available at https://doi.org/10.1038/s43017-022-00329-1.